




Local TLR4 stimulation augments in situ vaccination induced via local radiation and anti-CTLA-4 checkpoint blockade through induction of CD8 T-cell independent Th1 polarization

Justin C Jagodinsky ¹, Amber M Bates,¹ Paul A Clark ¹,
Raghava N Sriramaneni,¹ Thomas C Havighurst,² Ishan Chakravarty,¹
Erin J Nystuen,¹ KyungMann Kim,² Paul M Sondel ³, Won Jong Jin,¹
Zachary S Morris¹

To cite: Jagodinsky JC, Bates AM, Clark PA, *et al.* Local TLR4 stimulation augments in situ vaccination induced via local radiation and anti-CTLA-4 checkpoint blockade through induction of CD8 T-cell independent Th1 polarization. *Journal for ImmunoTherapy of Cancer* 2022;**10**:e005103. doi:10.1136/jitc-2022-005103

► Additional supplemental material is published online only. To view, please visit the journal online (<http://dx.doi.org/10.1136/jitc-2022-005103>).

Accepted 13 September 2022



© Author(s) (or their employer(s)) 2022. Re-use permitted under CC BY-NC. No commercial re-use. See rights and permissions. Published by BMJ.

For numbered affiliations see end of article.

Correspondence to

Dr Zachary S Morris;
zmorris@humonc.wisc.edu

Dr Won Jong Jin;
wjjin37@wisc.edu

ABSTRACT

Background Radiation therapy (RT) has been demonstrated to generate an in situ vaccination (ISV) effect in murine models and in patients with cancer; however, this has not routinely translated into enhanced clinical response to immune checkpoint inhibition (ICI). We investigated whether the commonly used vaccine adjuvant, monophosphoryl lipid A (MPL) could augment the ISV regimen consisting of combination RT and ICI.

Materials/methods We used syngeneic murine models of melanoma (B78) and prostate cancer (Myc-CaP). Tumor-bearing mice received either RT (12 Gy, day 1), RT+anti-CTLA-4 (C4, day 3, 6, 9), MPL (20 µg IT injection days 5, 7, 9), RT+C4+MPL, or PBS control. To evaluate the effect of MPL on the irradiated tumor microenvironment, primary tumor with tumor draining lymph nodes were harvested for immune cell infiltration analysis and cytokine profiling, and serum was collected for analysis of antitumor antibody populations.

Results Combination RT+C4+MPL significantly reduced tumor growth, increased survival and complete response rate compared with RT+C4 in both B78 and Myc-CaP models. MPL favorably reprogrammed the irradiated tumor-immune microenvironment toward M1 macrophage and Th1 TBET⁺CD4⁺ T cell polarization. Furthermore, MPL significantly increased intratumoral expression of several Th1-associated and M1-associated proinflammatory cytokines. In co-culture models, MPL-stimulated macrophages directly activated CD8 T cells and polarized CD4 cells toward Th1 phenotype. MPL treatment significantly increased production of Th1-associated, IgG2c antitumor antibodies, which were required for and predictive of antitumor response to RT+C4+MPL, and enabled macrophage-mediated antibody-dependent direct tumor cell killing by MPL-stimulated macrophages. Macrophage-mediated tumor cell killing was dependent on FcγR expression. In metastatic models, RT and MPL generated a systemic antitumor immune response that augmented response to ICIs. This was dependent on macrophages and CD4⁺ but not CD8⁺T cells.

WHAT IS ALREADY KNOWN ON THIS TOPIC

⇒ In situ vaccination strategies, particularly the combination of radiation and immune checkpoint blockade, have demonstrated promise in preclinical tumor models, however, response to such combinations remains limited in clinical settings.

WHAT THIS STUDY ADDS

⇒ Here, we demonstrate the capacity for an immune adjuvant, monophosphoryl lipid A (MPL), to enhance and shape the in situ vaccine effect elicited by the combination of radiation and immune checkpoint blockade by promoting Th1 and M1 polarization of CD4 T cells and macrophages in the irradiated tumor microenvironment, respectively, and by inducing production of antitumor antibodies that enable macrophage mediated tumor cell killing.

HOW THIS STUDY MIGHT AFFECT RESEARCH, PRACTICE OR POLICY

⇒ This study provides a readily translatable proof of concept that MPL, an immune adjuvant with demonstrated safety and efficacy in the setting of infectious disease vaccines, may augment and shape the response to an in situ anti-tumor vaccination.

Conclusions We report the potential for MPL to augment the ISV effect of combination RT+C4 through FcγR, macrophage, and TBET⁺CD4⁺ Th1 cell dependent mechanisms. To our knowledge, this is the first report describing generation of a CD8⁺ T cell-independent, Th1 polarized, systemic antitumor immune response with subsequent generation of immunologic memory. These findings support the potential for vaccine adjuvants to enhance the efficacy of in situ tumor vaccine approaches.

INTRODUCTION

The majority of patients with cancer will receive radiation therapy (RT) at some point

during their clinical care.¹ While previously thought of as primarily a cytotoxic therapy, growing evidence suggests that radiation has a variety of immunomodulatory effects within the tumor microenvironment. RT can induce immunogenic tumor cell death and release of tumor-specific antigens,^{2,3} and upregulation of immune susceptibility markers such as Fas and major histocompatibility complex (MHC) class I.^{4,5} Through these mechanisms, RT can help generate an in situ vaccination (ISV) effect converting the patient's own tumor into a nidus of enhanced antigen presentation in order to generate a more diverse tumor-specific T cell response that can be propagated to distant, out of RT field, sites of disease (ie, abscopal response).⁶⁻⁸

In contrast, radiation also induces changes within the tumor microenvironment that are potentially detrimental to the development of antitumor immunity. These can include blunting of effector immune cell infiltration within the tumor by recruiting suppressive regulatory T cells as well as increased infiltration and activation of inhibitory macrophage and myeloid-derived suppressor cell lineages.⁹⁻¹¹ Targeting such detrimental effects is one approach whereby immunotherapies may be used to augment the efficacy of radiotherapy.

Immune checkpoint inhibitors (ICIs) (eg, anti-PD-L1, and anti-CTLA-4) are a class of immunotherapies that modulate immune tolerance of a tumor by blocking specific inhibitory receptor–ligand interactions on the surface of immune cells and thereby overcoming T cell inhibition or exhaustion.¹² In patients with highly immunogenic tumors such as some melanomas, ICIs can restore efficacy to the antitumor immune response, sometimes resulting in complete and durable tumor regression even in settings of advanced metastatic disease.^{13,14} However, ICIs have not shown clinical benefit in the treatment of poorly immunogenic tumors such as prostate cancer that are characterized by low levels of T cell infiltrate and low mutation burden resulting in few mutation-created neoantigens.^{15,16} In addition, even patients with highly immunogenic tumors that initially respond to ICIs often exhibit disease progression over time.¹⁷

Several groups have taken advantage of the immunostimulatory effects of RT to improve response to ICI therapy with remarkable success in preclinical models.¹⁸⁻²¹ In addition, through mechanistic preclinical studies it is becoming increasingly clear that to generate clinically meaningful abscopal responses with RT, combination with immunotherapies such as ICI will likely be required.^{22,23} Early clinical studies combining RT with ICI have shown promise, however clinical responses remain limited.^{8,19,24,25} Therefore, there is immediate clinical need to boost both the rates and depth of response to combination RT and ICI therapy.

Monophosphoryl lipid A (MPL) is a derivative of the lipopolysaccharide (LPS) component of the cell wall of *Salmonella entericais*. MPL promotes immune activation in mice and humans through activation of toll-like receptor 4 (TLR4), with markedly reduced toxicity compared with

LPS.²⁶ Clinically, MPL is used as an adjuvant in several infectious disease vaccines including the hepatitis B virus (HBV) vaccine Fendrix²⁶ and the human papillomavirus (HPV) vaccine Cervarix.²⁷ Much like conventional vaccines, ISV regimens rely on promoting antigen recognition which may be enhanced through co-administration of adjuvants. Additionally, MPL may overcome further detrimental effects of RT that are not addressed with ICIs such as preventing the activation of inhibitory macrophage and myeloid-derived suppressor cell lineages. By promoting reprogramming of innate cell populations within the tumor microenvironment toward proinflammatory phenotypes, MPL may augment the antitumor response generated via combination RT and ICI and function as an adjuvant to ISV.

In this report, we evaluate the potential of MPL to function as an adjuvant to the in situ vaccine regimen of combination RT and anti-CTLA-4 in immunologically cold models of murine melanoma and prostate cancer. We demonstrate the capacity of intratumorally injected MPL to polarize CD4 T cells toward a Th1 phenotype, induce production of functional antitumor antibodies, and directly activate and polarize macrophages within the tumor microenvironment toward an M1 phenotype which enables macrophage mediated tumor cell direct killing through a Th1 CD4 T cell dependent mechanism, and promotes propagation of a systemic antitumor immune response independent of CD8 T cells.

MATERIALS AND METHODS

Study design

The objectives of this work were to determine whether the conventional vaccine adjuvant MPL could enhance the antitumor response of the ISV regimen consisting of combination RT and anti-CTLA-4, as well as determine mechanisms whereby MPL enhances antitumor efficacy. For our studies, tumors were established intradermally in mice, external beam radiation was delivered, phosphate-buffered saline (PBS) or anti-CTLA-4 were injected intraperitoneally, PBS or MPL were injected intratumorally, and tumor growth and overall survival were recorded. Serum was collected and analyzed for the presence and characterization of antitumor antibodies and the tumor and tumor draining lymph node were collected for immune infiltrate analysis. Mice were randomized to experimental groups/treatment the day before treatment initiation. Generally, experimental groups consisted of at least 5–6 mice, but in some experiments up to 10 were used. To determine the effects of MPL on immune cell populations we harvested macrophages from bone marrow and isolated CD4 and CD8 cells from spleens for *in vitro* monoculture and co-culture in the presence of MPL. To test which immune cell populations were critical for antitumor efficacy we used an antibody-mediated depletion of macrophages, NK cells, CD4, and CD8 T cells. To confirm the requirement for antitumor

antibodies to generate a sufficient antitumor immune response, we used mice deficient in Fc γ receptor.

Cell lines

The murine melanoma B78-D14 (B78) cell line, derived from B16 melanoma as previously described, was obtained from Ralph Reisfeld (Scripps Research Institute) in 2002.²⁸ The murine prostate cancer Myc-CaP cell line was obtained from American Type Culture Collection (ATCC). B78 and B16 cells were grown in RPMI-1640 and were supplemented with 10% fetal bovine serum (FBS), 100 U/mL penicillin, and 100 μ g/mL streptomycin. Myc-CaP cells were grown in DMEM and were supplemented with 10% FBS, 100 U/mL penicillin, and 100 μ g/mL streptomycin. Cell line authentication was performed per ATCC guidelines using morphology, growth curves, and Mycoplasma testing within 6 months of use.

Murine tumor models

Female C57BL/6, Fc γ R^{-/-} (Fc γ R deficient C57BL/6.129P2-Fcer1gtml1Rav N12), and male FVBn mice were purchased at age 6–8 weeks from Taconic. Female T-box transcription factor 21 (TBET) ^{-/-} (B6.129S6-Tbx21^{tm1Glm/J} strain #:004648) were purchased from The Jackson Laboratory. B78 and Myc-CaP tumors were engrafted by subcutaneous flank injection of 2 \times 10⁶ and 1 \times 10⁶ tumor cells, respectively. Tumor size was determined using calipers and volume approximated as (width² \times length)/2. Mice were randomized immediately before treatment when tumors were well-established (100–150 mm³), which occurred approximately 4 weeks after tumor implantation for B78 and 3 weeks for Myc-CaP. The day of radiation was defined as ‘day 1’ of treatment. In the case of the metastatic model, 250,000 B16 cells were injected via tail vein injection immediately following radiation. Anti-CTLA-4 (IgG2c, clone 9D9, produced by NeoClone) was administered by 200 μ g intraperitoneal injection on days 3, 6, and 9. MPL (Sigma Cat # SBR00012) was administered by 20 μ g intratumoral injection on days 5, 7, and 9. T-cell, NK cell, and macrophage depletion was performed as previously described.^{6,29} Depletion was confirmed on Day 15 of treatment (online supplemental figure S1). Mice were euthanized when tumor size exceeded 15 mm in longest dimension or whenever recommended by an independent animal health monitor for morbidity or moribund behavior.

Radiation

Delivery of RT *in vitro* was performed using a RS225 Cell Irradiator (Xstrahl). Delivery of RT *in vivo* was performed using an X-ray biological cabinet irradiator X-RAD 320 (Precision X-Ray). Mice were immobilized using custom lead jigs that exposed the right flank while shielding the rest of the mouse. In either case EBRT was prescribed to 12 Gy. The dose rate for RT delivery in all experiments was approximately 2 Gy/min. Dosimetric calibration and monthly quality assurance checks were performed

on these irradiators by University of Wisconsin Medical Physics Staff.

Serum antibody analysis

To assess for the presence of antitumor antibodies in treated mice, blood was collected at days 15 and 30 for analysis as previously described.³⁰ Briefly, serum components were isolated and frozen at -80°C until ready for analysis, at which point serum was thawed and co-incubated with B78 cells for antibody labeling. Labeled cells were washed and tumor bound antibody was detected using secondary antibodies [anti-mouse IgG-FITC (405305; Biolegend), anti-mouse IgG1-PE (406607; Biolegend), anti-mouse IgG2b-PE (406708; Biolegend), anti-mouse IgG2c-FITC (NBP2-68518; Novus)] and a live dead vitality stain (DAPI).

Cell culture

Macrophages were isolated from freshly harvested bone marrow as previously described.³¹ Briefly, isolated tibias were flushed with RPMI media and flowthrough was collected and centrifuged. The cell pellet was resuspended in RBC lysis buffer (Biolegend Cat # 420302) and filtered (70 μ M). Filtered cells were plated in non-tissue culture treated plates in Minimum Essential Medium Eagle - Alpha Modification (Alpha MEM) with Nucleosides supplemented with 10% FBS and 30 ng/mL macrophage colony-stimulating factor (M-CSF, Biolegend Cat # 576408). After 24 hours, the culture supernatant containing macrophages was harvested and plated in tissue culture treated plates in Alpha MEM supplemented with 10% FBS and 120 ng/mL M-CSF.

CD4 and CD8 T cells and B cells were isolated from freshly harvested spleens of naïve mice. Spleens were homogenized, filtered (70 μ M), and centrifuged. The cell pellet was resuspended in RBC lysis buffer and filtered (70 μ M). CD4, CD8, and B cells were sorted from total splenocytes using MACS column sorting (Miltenyi Biotec CD8a Cat # 130-104-075, CD4 Cat # 130-104-454, Pan B Cell Cat # 130-104-443) per manufacturer’s instructions.

To determine direct effects of MPL on macrophages, CD4 and CD8 T cells, and B cells, freshly isolated cells were cultured in 6-well plates containing Alpha MEM media (supplemented with 120 ng/mL M-CSF in the case of macrophages) in the presence of increasing amounts of MPL (5, 20, 100, and 500 ng/mL). After 24 hours, cells were harvested, and RNA was isolated for analysis via qPCR.

In vitro co-culture

Bone marrow derived macrophages were plated in 12 well plates (200,000 cells per well) containing Alpha MEM supplemented with 120 ng/mL M-CSF and treated with either 100 ng/mL MPL or PBS control. After 24 hours either CD4, CD8 or both were added (500,000 cells per well) to the culture. CD4 and CD8 cells were harvested 24 hours later and analyzed for activation markers using flow cytometry.

For co-culture with tumor cells, bone marrow derived macrophages (harvested from wild-type or Fc γ receptor deficient C57BL/6 mice) were plated in 6 well plates (500,000 cells per well) containing Alpha MEM supplemented with 120 ng/mL M-CSF and treated with either 100 ng/mL MPL or PBS control. After 24 hours either B78 melanoma or Myc-CaP cells were added (200,000 cells per well). To test whether serum derived antitumor antibodies can activate macrophages, 5 μ L of serum obtained from mice bearing B78 tumors rendered disease free was also added to the co-culture. After 24 hours cells were harvested and analyzed for polarization and activation markers using qPCR.

Cell killing assay

Bone marrow derived macrophages (harvested from wild-type or Fc γ receptor deficient C57BL/6 mice) were plated in 48 well plates (400,000 cells per well) containing Alpha MEM supplemented with 120 ng/mL M-CSF and treated with either 100 ng/mL MPL or PBS control. After 24 hours B78 melanoma cells were added (20,000 cells per well, 20:1 effector to target ratio) with or without 5 μ L of serum obtained from mice bearing B78 tumors rendered disease free. After 24 hours cells were harvested via gentle scraping and washed with PBS twice. For cytotoxic CD4 T cell assessment, CD4 cells were isolated from spleens of B16 tumor bearing mice treated with either RT+C4+MPL or PBS control on day 15 following treatment and co-cultured with B16 cells that had received 0 or 12 Gy of RT. After 24 hours cells were harvested via gentle scraping and washed with PBS twice. In either case, a single cell suspension was labeled with CD45 antibody (anti-CD45-PE-Cy7, BioLegend, 157206) at 4°C for 30 min and washed three times using flow buffer (2% FBS+2 mM EDTA in PBS). The single cell suspension was then labeled with the apoptotic marker Annexin V using the FITC Annexin V/Dead Cell Apoptosis Kit, (ThermoFisher Scientific Cat # V13242) per manufacturer's instructions. Flow cytometry was performed using an Attune NxT Flow Cytometer (ThermoFisher). Data was analyzed using FlowJo Software and percent of CD45⁺ Annexin V⁺ cells was quantified.

Gene expression analysis

Cells treated *in vitro* with MPL, RT, or the combination were washed with cold PBS, TRIzol reagent (ThermoFisher Scientific Cat # 15596026) was added to the plate, and the cells were collected via scraping over ice. For analysis of tumor tissue, tumors were harvested, and samples were homogenized in TRIzol using a Bead Mill Homogenizer (Bead Ruptor Elite, Omni International Cat # 19-040E). For *in vitro* and *in vivo* samples, total RNA was extracted using RNeasy Mini Kit (QIAGEN, Germany, Cat # 74106) according to the manufacturer's instructions. Extracted RNA was subjected to complementary cDNA synthesis using QuantiTect Reverse Transcription Kit (QIAGEN, Germany, Cat # 205314) according to the manufacturer's instructions. Quantitative PCR (qRT-PCR)

was performed using Taqman Fast Advanced qPCR Master Mix (ThermoFisher Scientific Cat # 4444556) or PowerUp SYBR Green Master Mix (ThermoFisher Scientific Cat # A25741). Thermal cycling conditions (Quantstudio 6, Applied Biosystems) included the UDG activation at 50°C for 2 min, followed by Dual-Lock DNA polymerase activation stage at 95°C for 2 min followed by 40 cycles of each PCR step (denaturation) 95°C for 1 s and (annealing/extension) 60°C for 20 s. A melt curve analysis was done to ensure specificity of the corresponding qRT-PCR reactions. For data analysis, the Ct values were exported to an Excel file, and fold change normalized to untreated control samples was calculated using the $\Delta\Delta$ Ct method. *Hprt*, was used as endogenous controls. A complete list of Taqman probes and primers is included as online supplemental table S1.

Flow cytometry

Flow cytometry was performed as previously described,³² using fluorescent beads (UltraComp Beads eBeads, 176 Invitrogen, #01-2222-42) to determine compensation and fluorescence minus one methodology to determine gating (online supplemental figure S2). For *in vivo* analysis, tumors and tumor draining lymph nodes were harvested and gently dissociated. For *in vitro* analysis, nonadherent CD4 and CD8 cells were collected from culture plates and washed with PBS twice. B16 tumor cells or macrophages were washed with PBS and collected via gentle scraping. In either case total cells were treated CD16/32 antibody (BioLegend) to prevent non-specific binding. Live cell staining was performed using Ghost Red Dye 780 (Tonbo Biosciences) according to manufacturer's instruction. After live-dead staining, a single cell suspension was labeled with the surface antibodies at 4°C for 60 min and washed three times using flow buffer (2% FBS+2 mM EDTA in PBS). For intracellular staining, the cells were fixed and stained for internal markers with permeabilization solution according to manufacturer's instructions (BD Cytotfix/CytopermTM). Flow cytometry was performed using an Attune NxT Flow Cytometer (ThermoFisher). Data were analyzed using FlowJo Software. Complete list of antibody targets, clones, and fluorophores is provided as online supplemental figure S2.

Tumor cytokine multiplex immunoassay

At day 15, tumors were harvested and weighed. Tumor samples (5 μ L/mg) were lysed in 20% Cell Lysis Buffer with phenylmethylsulfonyl fluoride (PMSF) (Cell Signaling Technology) and supplemented with Halt Protease and Phosphatase Inhibitor Cocktail (Thermo Scientific). Each tumor was homogenized in bead beater tubes, and the lysate was stored at -80°C. The concentration of 32 cytokines and chemokines in the tumor lysates (MILLIPLEX MAP Mouse Cytokine/Chemokine Magnetic Bead Panel, Millipore) were determined by a multiplex immunoassay following manufacturer's instructions. The MAGPIX System (Millipore) was used to read the multiplex plate. Concentrations were determined

using a standard curve and their respective median fluorescence intensity readings (Milliplex Analyst, Millipore). The data underwent log and Z-transformation followed by unbiased hierarchical clustering.

Statistical analysis

Prism V.8 (GraphPad Software) and R V.4.0.2 (The R Foundation) were used for all statistical analyses. One-way analysis of variance with Tukey's honestly significant difference test to adjust for multiple comparisons was used to assess statistical significance of observed mean differences in gene expression and immune cell quantification. For comparisons between two groups a Student's t-test was performed. For tumor growth analysis, a linear mixed model after log transformation of tumor volume was fitted on treatment and day. Day and the interaction between treatment and day were fixed effects. When testing differences in slopes of log-transformed tumor volume, a Tukey adjustment for multiplicity was used. The Kaplan-Meier method was used to estimate the survival distribution for the overall survival. A Cox regression model was fitted, and pairwise comparison of the overall survival was made using a log-rank test with Benjamini-Hochberg adjustment of p values between levels of factors. χ^2 test was used to compare complete response (CR) rate. All data presented are reported as mean \pm SEM unless otherwise noted. For all graphs, *, p<0.05; **, p<0.01; ***, p<0.001; and ****, p<0.0001.

RESULTS

Intratumoral MPL enhances antitumor response generated by combination RT and anti-CTLA-4

We tested the capacity of MPL to function as an adjuvant to combination therapy consisting of RT and anti-CTLA-4 in mice bearing B78 melanoma. We randomized mice to receive either RT (12Gy delivered on day 1), RT+anti-CTLA-4 (C4; 200 μ g intraperitoneal injection on days 3, 6, 9), RT+C4+MPL (20 μ g intratumoral injection on days 5, 7, 9), RT+MPL, MPL+C4, C4 alone, MPL alone, or PBS control (figure 1A). The MPL dosing regimen was chosen to coincide with pre-peak, peak, and postpeak immune activation using type 1 interferon induction as a marker following RT in our model with peak expression occurring 7 days following RT.³³ For reference, the full factorial dataset is included as a supplement (online supplemental figure S3) with key comparison groups displayed in figure 1. We observed a significant reduction in tumor volume with combination RT+C4+MPL compared with single agent treatment groups (PBS vs RT+C4+MPL p<0.001; RT vs RT+C4+MPL p<0.001; MPL vs RT+C4+MPL p<0.001) (figure 1B,C). This resulted in a significant increase in overall survival (PBS vs RT+C4+MPL median survival 31 days vs UND, p<0.001; RT vs RT+C4+MPL median survival 31 days vs UND, p<0.001; MPL vs RT+C4+MPL median survival 31 days vs UND, p<0.001) (figure 1D). Compared with RT+C4, combination RT+C4+MPL resulted in a significant reduction in

tumor volume (p=0.003) and increase in overall survival (RT+C4 vs RT+MPL+C4 median survival 44 days vs UND, p=0.002) (figure 1B–D). Moreover, the addition of MPL significantly increased the CR rate generated by combination RT+C4 (RT+C4 vs RT+MPL+C4 CR% 12.5% vs 44%) (figure 1E). In both RT+C4 and RT+C4+MPL treatment groups, mice that were rendered disease free rejected rechallenge with B78 cells, demonstrating development of a specific antitumor immune response (figure 1F).

We then sought to test our combination treatment strategy in a separate model of prostate cancer. In contrast to melanoma, prostate tumors commonly arise from driver mutations or oncogenic translocations and these tumors have a low mutation burden, limited antitumor immune response, and poor response to ICIs^{34,35} even when delivered in combination with RT.¹⁶ We confirmed these findings using the syngeneic Myc-CaP prostate cancer model. Combination RT+C4 failed to significantly reduce tumor growth compared with RT alone (p=0.094) or PBS control (p=1). In contrast, we observed a significant reduction in tumor volume (p<0.001) and increase in overall survival (RT+C4 vs RT+MPL+C4 median survival 23.5 days vs UND, p=0.017) with the addition of MPL to RT+C4 (figure 1G–I). In addition, we observed an increase in CR rate (RT+C4 vs RT+MPL+C4 CR% 16.7% vs 50%) which trended toward significance (p=0.0833) (figure 1J). Mice rendered disease free at day 90 following treatment rejected rechallenge, confirming immunological memory (figure 1K).

MPL polarizes toward Th1 phenotype and is predictive of response to ISV

To test whether MPL polarizes CD4 cells to a Th1 phenotype in a radiated tumor microenvironment, we treated mice bearing B78 tumors with either PBS, RT, RT+C4, RT+C4+MPL, or MPL alone and collected serum at day 15 and 30 following RT. We incubated B78 cells with serum and then quantified levels of select IgG subclasses using fluorescently labeled secondary antibodies (anti-IgG, anti-IgG1, anti-IgG2c) via flow cytometry (figure 2A). In C57BL/6 mice the antibody class IgG2c is associated with Th1 polarization whereas IgG1 is associated with Th2 polarization.³⁶ Using IgG2c:IgG1 as a marker of Th1 polarization, we observed a statistically significant increase in the IgG2c:IgG1 ratio in the RT+C4+MPL group compared with all others at day 15 following treatment (figure 2B, online supplemental figure S4). We found that the total anti-B78 IgG antibody population was unchanged by treatment, when measured at day 15 (figure 2C). At day 30, the IgG2c:IgG1 ratio further increased by 100-fold compared with day 15, with RT+C4+MPL demonstrating the highest ratio compared with other groups which trended toward significance (figure 2D). We also found that the total anti-B78 IgG antibody population was unchanged by treatment, when measured at day 30 (figure 2E).

To determine whether the antibody class ratios correlated with depth of response, we classified the serum

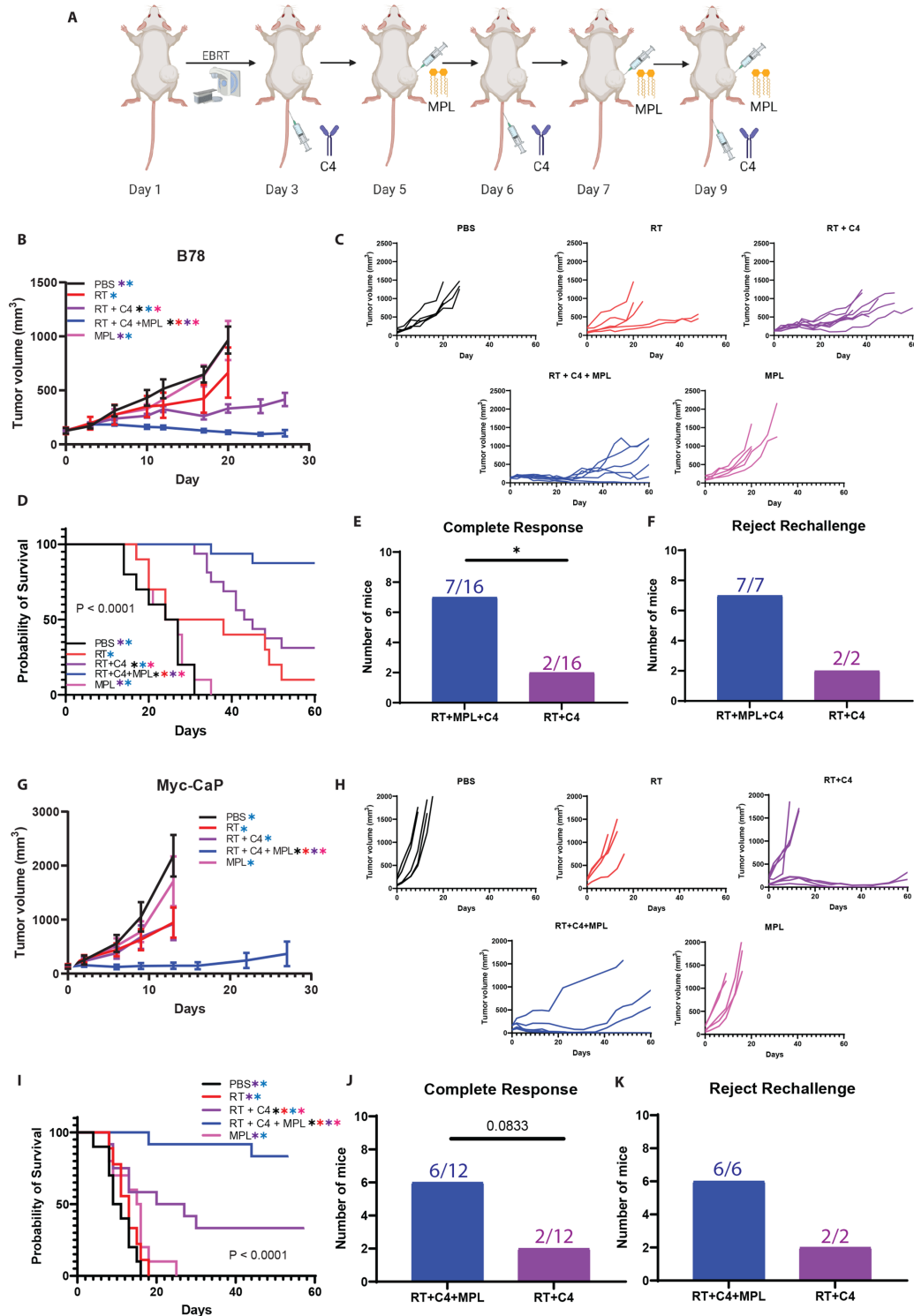


Figure 1 MPL enhances efficacy of RT+C4 in B78 melanoma and Myc-CaP prostate cancer models. (A) Mice with a single B78 or Myc-CaP flank tumor were treated with PBS, external beam radiation (RT, 12 Gy), RT+anti-CTLA-4 (C4, 200 µg), RT+C4+MPL (Mpl, 20 µg), or MPL alone. Tumor response, by group, by individual animal, and animal survival are shown for B78 (in B), (C, D). Mice with complete response to treatment with either RT+C4 or RT+C4+MPL (E) were rechallenged with the same tumor they initially rejected (F). Tumor response, by group, by individual animal, and animal survival are shown for Myc-CaP (in G), (H, I). Mice with complete response to treatment with either RT+C4 or RT+C4+MPL (J) were rechallenged with the same tumor they initially rejected (K). n=10–16 mice per group. Significance determined by linear mixed effects regression analysis with Tukey multiple comparisons testing for tumor growth (significant differences, $p < 0.05$, demarcated by * with the color of the asterisk representing which group from which the sample is significantly different), Kaplan-Meier estimation with log-rank testing and Cox regression for survival analysis (significant differences, $p < 0.05$, demarcated by * with the color of the asterisk representing which group from which the sample is significantly different), and χ^2 test for complete response rate. MPL, monophosphoryl lipid; RT, radiation therapy; EBRT, external beam radiation therapy; PBS, phosphate buffered saline.

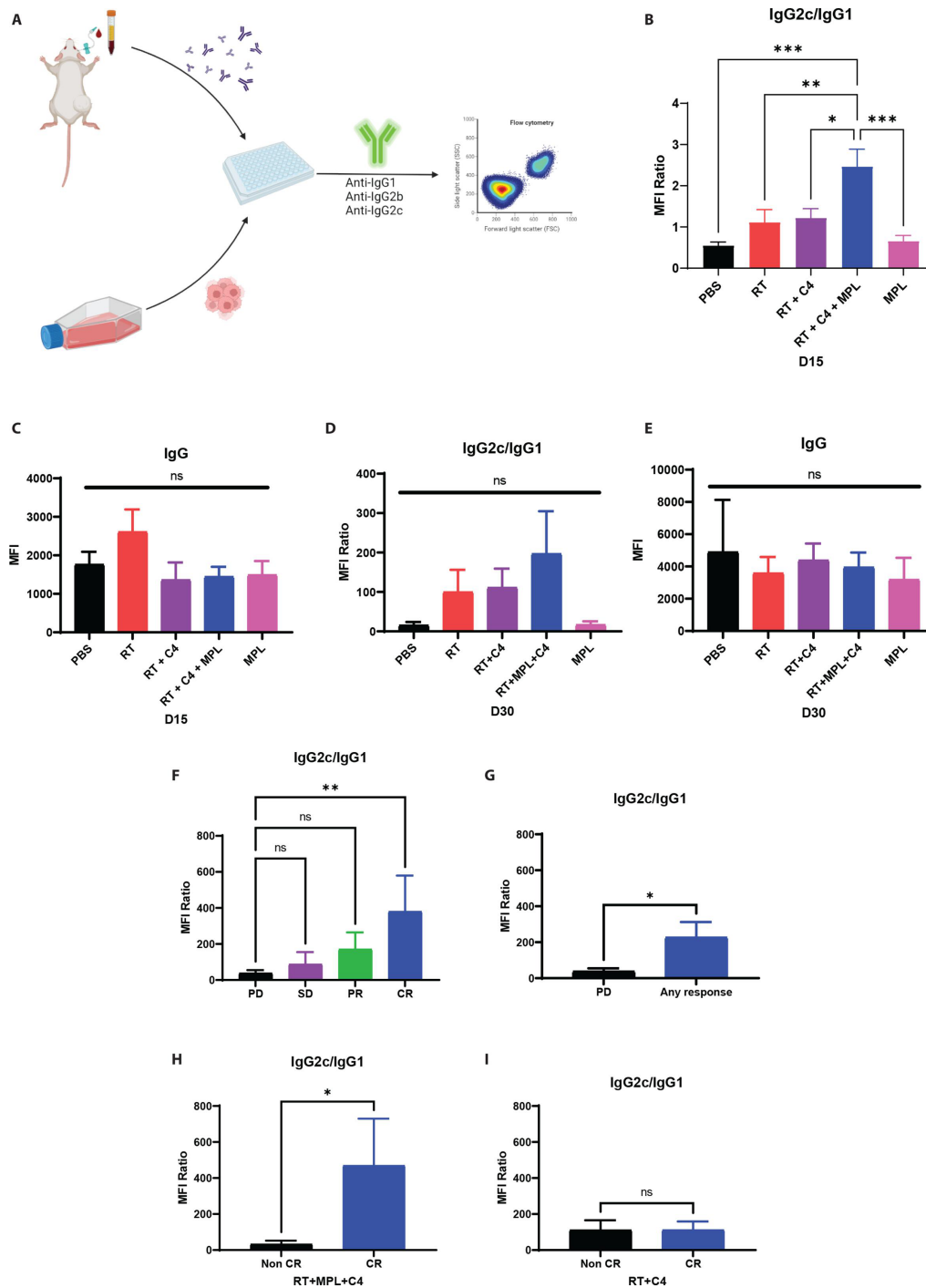


Figure 2 MPL promotes Th1 antibody class switching and correlates with depth of tumor response. To determine the presence of antitumor antibodies serum was isolated from mice bearing B78 tumors at days 15 and 30 following treatment initiation. Serum was incubated with B78 cells and antibody class was determined using secondary antibodies against IgG, IgG₁, and IgG2c (A). Ratio of IgG2c:IgG1 at D15 was increased in RT+C4+MPL compared with other groups without a change in overall IgG (B, C). Similar trends in IgG2c:IgG1 ratio were observed at day 30; however, did not reach statistical significance (D, E). In a treatment agnostic fashion, mice were reclassified based on depth of response using RECIST criteria 1.1 [PD: progressive disease N=33, SD: stable disease N=6, PR: partial response N=7, CR: complete response N=9] and ratio of IgG2c:IgG1 was quantified (F). Mice experiencing any response (SD, PR or CR, N=22) were also pooled and the IgG2c:IgG1 ratio was compared with nonresponding mice (PD, N=33) (G). Within treatment groups that had mice experiencing a complete response (RT+C4 and RT+C4+MPL) the IgG2c:IgG1 was quantified in mice experiencing a complete response (RT+C4, N=2 and RT+C4+MPL, N=7) and was compared with nonresponding mice (RT+C4, N=14 and RT+C4+MPL, N=9). The IgG2c:IgG1 ratio was elevated in complete responding mice treated with RT+C4+MPL (H) but not RT+C4 (I). One-way ANOVA with Tukey's honestly significant difference (HSD) test to adjust for multiple comparisons was used to assess statistical significance of observed mean differences in IgG2c:IgG1 ratio (significant differences, * $p < 0.05$, ** $p < 0.01$, *** $p < 0.001$, **** $p < 0.0001$). For comparisons between two groups a Student's t-test was performed. ANOVA, analysis of variance; MPL, monophosphoryl lipid.

antibody populations by Response Evaluation Criteria in Solid Tumors (RECIST) criteria in a treatment agnostic manner. The IgG2c:IgG1 ratio was significantly increased in responding mice compared with mice with progressive disease, with the highest ratio in the CR group and second highest in the partial response group (figure 2F). In the RT+MPL+C4 group, mice with a CR had a significant increase in IgG2c/IgG1 compared with nonresponders (figure 2G), which likely underlies the loss of statistical significance comparing RT+MPL+C4 to other groups (figure 2D). This association of IgG2c:IgG1 ratio with CR was not seen in the RT+C4 group suggesting that the addition of MPL increases the CR rate in a Th1 mediated fashion (figure 2H).

MPL polarizes macrophages toward M1 phenotype, and promotes T cell activation

We next sought to determine the effects of MPL on the irradiated tumor immune microenvironment. We randomized B78 tumor bearing mice to either PBS, RT, RT+C4, RT+C4+MPL, or MPL alone and harvested tumors and the tumor draining lymph node on day 15 following RT. We observed a significant difference in number of macrophages in the RT+C4+MPL group compared with RT alone (figure 3A). Combination RT+C4 significantly increased the percentage of antitumor M1 macrophages (F4/80⁺CD11b⁺CD80⁺) out of total macrophages (CD11b⁺F480⁺) compared with PBS, RT, and MPL groups. This increase was further enhanced with the addition of MPL (figure 3B). In addition, the percentage of M2 macrophages (F4/80⁺CD11b⁺CD206⁺) out of total macrophages (CD11b⁺F480⁺) was significantly decreased in the RT+C4+MPL group compared with PBS, RT+C4 and MPL groups (figure 3C). This resulted in a significant increase in the M1:M2 ratio in the RT+C4+MPL group compared with all others (figure 3D). In addition, we observed a significant increase in number of CD8 T cells present in the tumor in both the RT+C4 and RT+C4+MPL groups compared with PBS control (figure 3E).

We then sought to determine whether MPL influenced antigen presentation in the context of the irradiated tumor immune microenvironment and to characterize CD4 Th populations in order to corroborate our anti-tumor antibody characterization findings following MPL treatment. Within the tumor draining lymph node we observed comparable increases in type 1 dendritic cells between RT+C4 and RT+C4+MPL, which were both significantly increased compared with PBS, RT, and MPL (figure 3F). The percentage of Th1 cells (CD4⁺TBET⁺) was significantly increased in the RT+C4+MPL group compared with all others, which is consistent with the increase in Th1-associated IgG2c antibody class switching we observe following RT+C4+MPL treatment (figure 3G). We observed significant increases in CD103⁺ CD4⁺ memory T cells in RT+C4 compared with PBS, RT, and MPL. This was further enhanced with the addition of MPL (figure 3H). Additionally, RT+C4+MPL generated significant increases in IFN γ ⁺ CD8 T cells and CD103⁺

CD8⁺ memory T cells compared with all other groups (figure 3I,J).

We next profiled the cytokine repertoire within the irradiated tumor immune microenvironment following MPL treatment, focusing on TLR4 activation, Th polarization, and macrophage polarization given our tumor immune cell infiltration findings. We observed significant increases in keratinocytes-derived chemokine (KC, CXCL1) and macrophage inflammatory protein 2 (MIP2, CXCL2) in both RT+C4+MPL and MPL groups (figure 3K,L), consistent with TLR4 signaling activation.³⁷ RT+C4+MPL significantly increased expression of Th1 associated cytokines IL-12 compared with all other groups and IL-2 compared with all other groups except RT+C4 which trended toward significance (figure 3M). RT+C4 favored Th2 signaling and led to significant increases in Th2 cytokines IL-4 and IL-5 compared with all other groups (figure 3N). Lastly, RT+C4+MPL significantly increased several proinflammatory cytokines associated with M1 polarization including IL-1 α , IL-1 β , LPS-induced CXC chemokine (LIX, CXCL5), TNF α , and GM-CSF compared with all other groups (figure 3O).

MPL induces CD8 T cell activation through direct stimulation and M1 polarization of macrophages

Given our observations that MPL significantly altered the infiltration and polarization of macrophages, CD4, and CD8 T cells within the irradiated tumor immune microenvironment, we sought to determine the direct effects of MPL on these populations. We cultured bone marrow derived macrophages in the presence of increasing amounts of MPL and using qPCR quantified the expression of *Arg1* and *Nos2*, markers of M2 and M1 macrophages, respectively. We observed dose dependent increases in both *Arg1* and *Nos2*, with significantly greater expression of *Nos2* than *Arg1* at the 100 and 500 ng/mL doses, strongly favoring M1 polarization (figure 4A). We observed similar trends with MPL favoring expression of proinflammatory cytokines (figure 4B) compared with anti-inflammatory cytokines (figure 4C).

We then tested whether *in vitro* MPL treatment can directly polarize naïve splenic CD4 T cells. Using *Cxcr3* and *Cxcr4* as markers of Th1 and Th2 cells, respectively, we observed minimal changes in *Cxcr3* and *Cxcr4* expression indicating MPL treatment does not directly influence CD4 T cell polarization (figure 4D). When MPL was added to CD4 and CD8 cells in culture we again observed minimal increases in expression of proinflammatory cytokines, suggesting MPL does not have a direct effect on T cell activation (figure 4E,F).

We hypothesized that MPL may favorably polarize and activate T cells through direct activation of macrophages. To test this, we co-cultured CD8 cells with macrophages stimulated with MPL or vehicle control (PBS) and quantified CD69 expression as a marker of activation. We observed that macrophages stimulated with MPL significantly increased expression of CD69 on CD8 T cells compared with CD8 T cells in monoculture or CD8 T cells

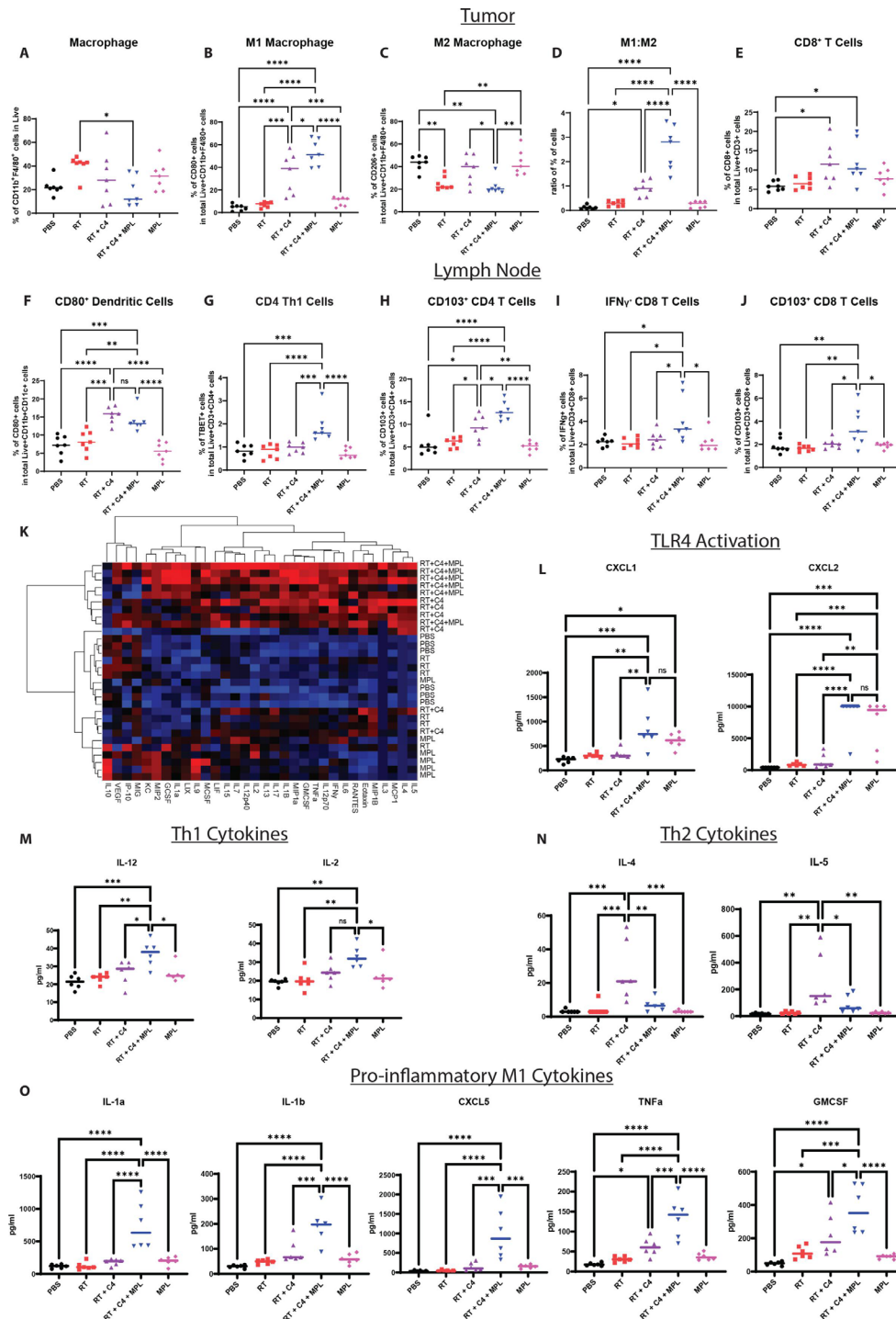


Figure 3 MPL reprograms the immune microenvironment to favor M1 and Th1 polarization. Flow cytometry analyses of tumor immune cell infiltrates [total macrophages (CD11b⁺F4/80⁺), M1 macrophages (CD80⁺), M2 macrophages (CD206⁺), ratio of M1:M2 macrophages, and CD8⁺ T cells (CD8⁺)] (A–E) and lymph node immune populations [classical dendritic cells (CD11c⁺CD103⁺MHC-II⁺CD80⁺), Th1 cells (TBET⁺CD4⁺), resident memory CD4 T cells (CD4⁺CD103⁺), IFN γ producing CD8 T cells (CD8⁺Ifn γ ⁺), and resident memory CD8 T cells (CD8⁺CD103⁺)] (F–J) as a percent of total live cells is shown at day 15 following treatment initiation in B78 melanoma. N=7 mice per group. (K) Tumors from a separate cohort of mice were subjected to cytokine profiling. Cytokine and chemokine concentrations in tumor lysates were measured by multiplex immunoassay. Hierarchical clustering analysis was performed, and the assay results were displayed as a Z-score for each cytokine or chemokine. The addition of MPL to RT+C4 increases expression of TLR4-associated cytokines (L), increases Th1 cytokines (M), decreases Th2 cytokines (N), and increases several proinflammatory M1 cytokines compared with RT+C4 (O). N=6 mice per group. One-way ANOVA with Tukey's honestly significant difference (HSD) test to adjust for multiple comparisons was used to assess statistical significance of observed mean differences in immune cell populations and cytokine secretion (significant differences, *p<0.05, **p<0.01, ***p<0.001, ****p<0.0001). CR, complete response; MFI, median fluorescence intensity; MPL, monophosphoryl lipid; RT, radiation therapy.

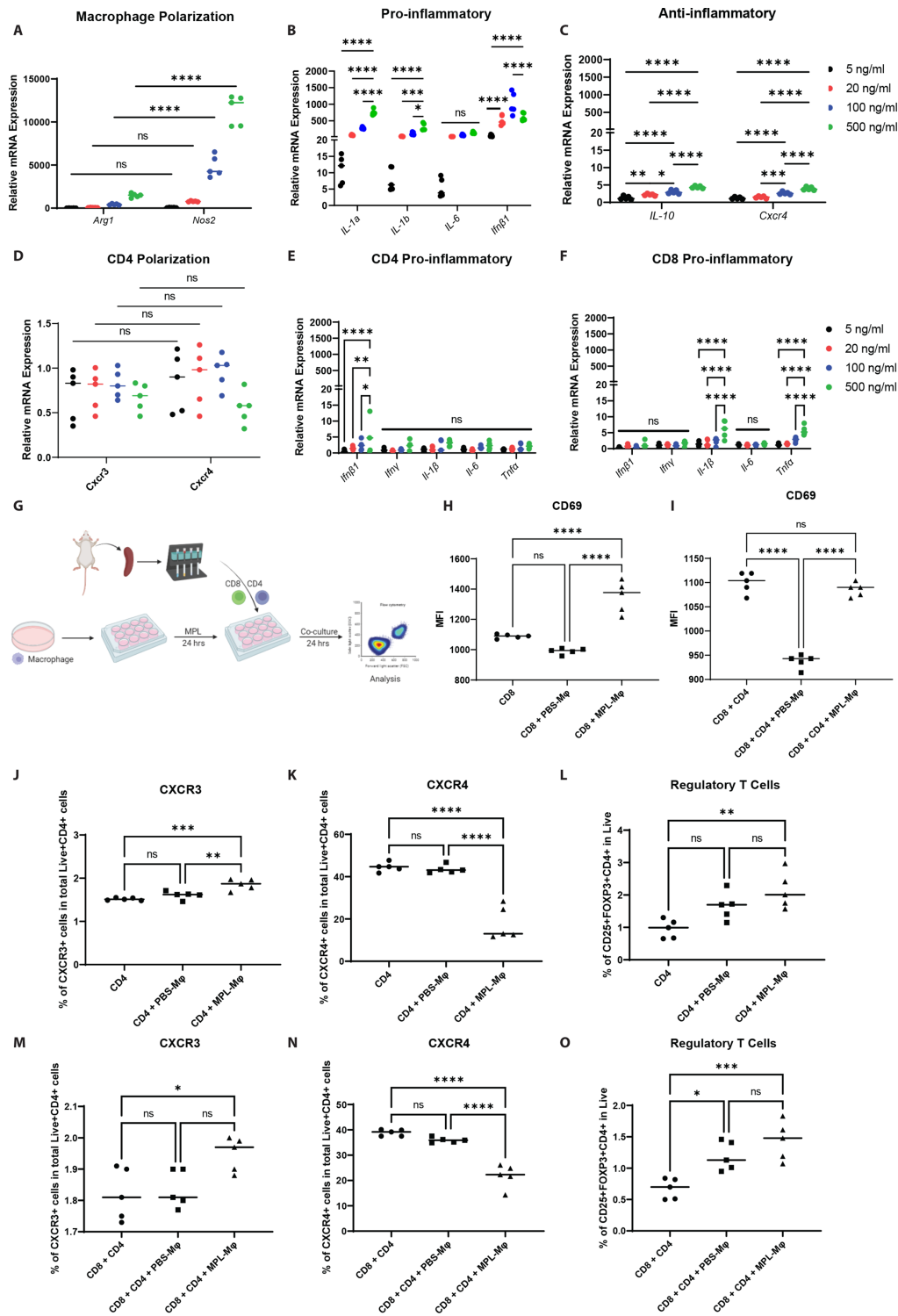


Figure 4 MPL directly activates macrophages to influence polarization of Th cells. Bone marrow derived macrophages were cultured in the presence of increasing amounts of MPL (0, 5, 20, 100, 500 ng/mL) and 24 hours later were harvested for qPCR analysis to quantify polarization (A), proinflammatory cytokines (B), and anti-inflammatory markers (C). This was repeated with freshly isolated CD4 and CD8 cells from mouse spleens to determine CD4 polarization (D), activation (E), and CD8 activation (F) following MPL treatment. The potential for MPL stimulated macrophages to activate CD8 T cells and polarize CD4 T cells was determined using a co-culture system (G). MPL stimulated macrophages increase activation of CD8 T cells (CD69⁺) when co-cultured (H), but not when in the presence of CD4 T cells (I). MPL stimulated macrophages increase Th1 polarization (CXCR3⁺) (J), decrease Th2 polarization (CXCR4⁺) (K), and increase regulatory T cell polarization (CD25⁺FOXP3⁺) (L) when co-cultured. Identical trends were observed with the addition of CD8 T cells (M–O). One-way ANOVA with Tukey's honestly significant difference (HSD) test to adjust for multiple comparisons was used to assess statistical significance of observed mean differences in gene expression (significant differences, * $p < 0.05$, ** $p < 0.01$, *** $p < 0.001$, **** $p < 0.0001$). $N = 5$ replicates per group. ANOVA, analysis of variance; MPL, monophosphoryl lipid.

cultured with unstimulated macrophages (figure 4H). Interestingly, when CD4 cells were added to the culture, we no longer observed an increase in CD69 expression on the CD8 cells (figure 4I). To investigate CD4 polarization, we co-cultured CD4 cells with macrophages stimulated with MPL or PBS. We observed a significant increase in CXCR3 expression and decrease in CXCR4 expression in CD4 cells co-cultured with stimulated macrophages (figure 4J,K). Interestingly, we also observed a significant increase in the percentage of regulatory T cells (CD4⁺CD25⁺FOXP3⁺) when CD4 T cells were cultured with activated macrophages (figure 4L). This may partially explain the loss of CD69 expression in CD8 T cells when CD4 T cells were added to the co-culture. We observed similar trends in CXCR3 and CXCR4 expression on CD4⁺ cells, as well as increase in regulatory T cell percentage when CD8 T cells were added to the co-culture (figure 4M–O).

Radiation and antitumor antibodies synergize with MPL treatment to activate macrophages

Tumor-associated macrophage populations that receive radiation in this regimen likely survive and are subsequently exposed to MPL delivered intratumorally as part of our treatment strategy. To test whether RT can synergize with MPL to further increase activation of macrophages, we delivered 12 Gy of RT to macrophages in culture and immediately replaced the growth media with fresh media containing 100 ng/mL of MPL, and 24 hours later harvested cells for analysis. We observed that the addition of RT to MPL further increased the expression of proinflammatory marker *Ifnβ1* as well as M1 marker *Nos2* compared with MPL treatment alone (figure 5A). Interestingly, RT had no effect on expression of TLR4 on macrophages, suggesting the enhanced activation extends beyond MPL-TLR4 receptor binding (online supplemental figure S5A).

Given our observations that MPL can activate and favorably polarize macrophages, CD8, and CD4 T cells, we next sought to determine whether the antitumor antibodies generated via combination RT+C4+MPL contributed to the observed immune cell activation or functioned solely as a predictive biomarker of CR. We harvested serum on day 30 following RT from mice bearing B78 melanoma tumors that were rendered disease free following combination RT+C4+MPL treatment. We cultured bone marrow derived macrophages, alone (mono) or in co-culture with B78 cells, in the presence of MPL and/or serum from mice bearing B78 tumors that were rendered disease-free following RT+MPL+C4 (figure 5B). In macrophages grown in monoculture, we again observed significant increases in *Arg1* and *Nos2* expression with the addition of MPL heavily favoring *Nos2* expression. The addition of serum did not significantly increase expression of either gene, nor did the addition of serum to MPL stimulated macrophages further increase expression compared with MPL stimulation alone (figure 5C). Similar trends were observed with activation markers *Il-1a* and *Ifnβ1* (figure 5D). When macrophages were co-cultured with

B78 cells we observed a significant increase in expression of *Nos2* but not *Arg1* following MPL treatment. Treatment with serum alone did not significantly increase expression of either gene. However, when serum was added to macrophages stimulated with MPL we observed further significant increases in expression of both *Arg1* and *Nos2* with the addition of MPL favoring *Nos2* expression (figure 5E). Similar trends to those seen with *Nos2* were observed with activation markers *Il-1a* and *Ifnβ1* (figure 5F). This suggests that antitumor antibodies can further increase activation of macrophages stimulated with MPL, but only in the presence of tumor cells. We confirmed that the effects of serum in this co-culture experiment were tumor cell specific using a control study in which macrophages were co-cultured with Myc-CaP cells that are unrelated to the B78 tumors that had been eradicated by RT+MPL+C4 in mice from whom serum was drawn. When macrophages were co-cultured with Myc-CaP cells and serum from mice rendered disease free from a B78 melanoma tumor by RT+MPL+C4, we observed no increase in the expression of macrophage polarization or activation markers with the addition of serum compared with MPL treatment alone (figure 5G,H).

Given that serum only had activating effects in the context of MPL treatment, we hypothesized that MPL enhances binding and recognition of antitumor antibodies bound to tumor cells. To test this, we first compared the antitumor efficacy of combination RT+C4+MPL in wild-type and FcγR^{-/-} mice. FcγR deficiency abrogated the antitumor response and survival benefit of RT+C4+MPL compared to wild-type mice (figure 6A,B). We then further explored the effects of RT and MPL on bone marrow derived macrophages cultured *in vitro*. We delivered 12 Gy of RT to macrophages in culture and immediately replaced the growth media with fresh media containing 100 ng/mL of MPL, and 24 hours later harvested cells for analysis. We observed that MPL treatment significantly increased expression of activating FcγR1 and FcγR4 as well as inhibitory FcγR2. The addition of radiation to the MPL further increased expression of these Fcγ receptors with FcγR1 and FcγR4 significantly increased compared with the increase seen for FcγR2 (figure 6C). To confirm that the observed synergistic activation of macrophages with MPL and serum relied on FcγR expression, we cultured bone marrow derived macrophages deficient in Fcγ receptor in mono and co-culture with B78 cells in the presence of MPL and/or serum. In FcγR^{-/-} macrophages grown in monoculture, we again observed significant increases in *Arg1* and *Nos2* expression with the addition of MPL heavily favoring *Nos2* expression. The addition of serum further increased expression of *Arg1* but not *Nos2*, *Il-1a*, or *Ifnβ1* (figure 6D,E), somewhat similarly to that observed for wild-type macrophages (figure 5C,D, figure 6D,E). When FcγR^{-/-} macrophages were co-cultured with B78 cells we observed a significant increase in expression of *Nos2* but not *Arg1* following MPL treatment similar to what we observed with wild-type macrophages. In contrast to wild-type macrophages, the addition of serum in the

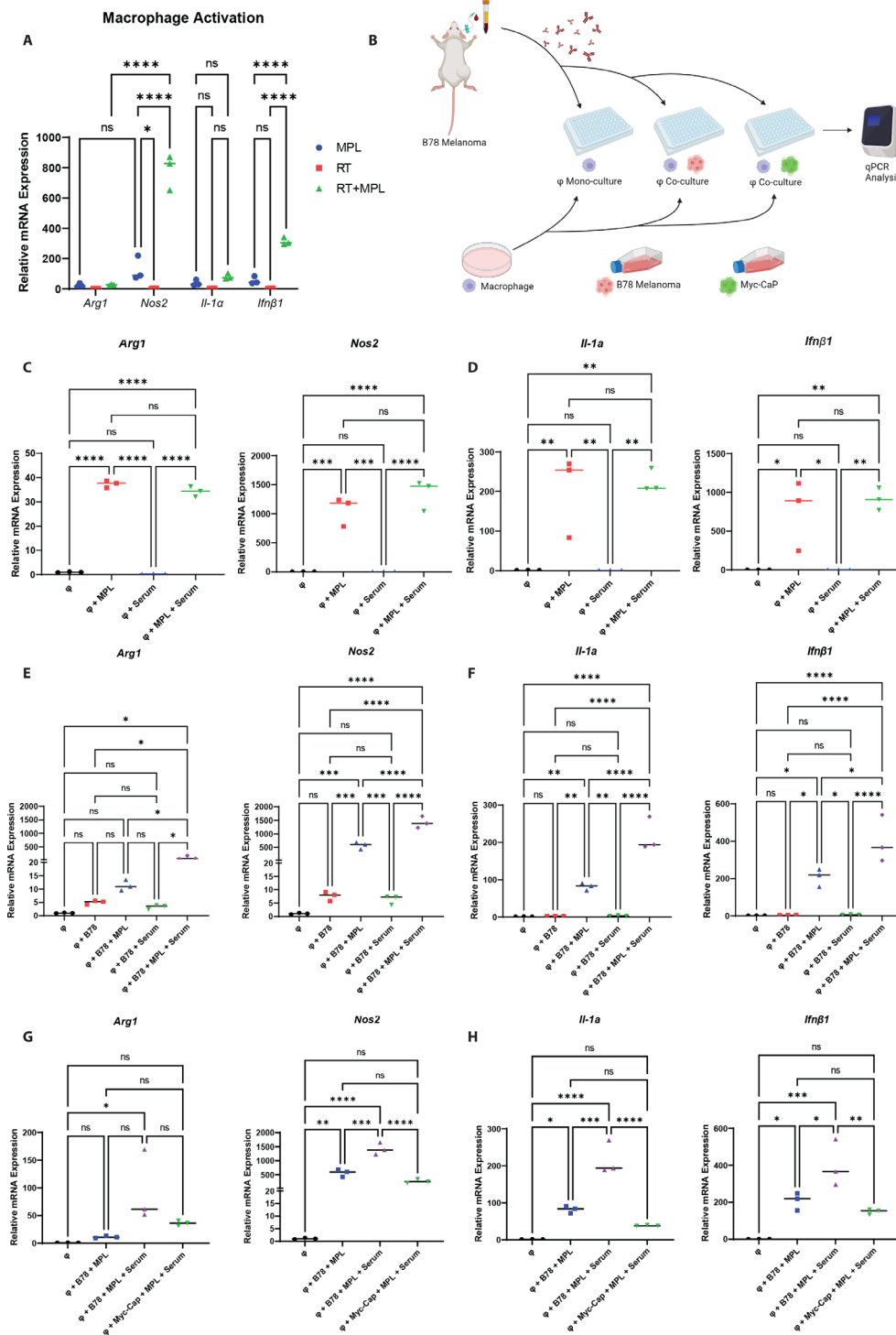


Figure 5 Serum antibody bound to tumor cells enhances MPL-induced activation of macrophages. Bone marrow derived macrophages were radiated in culture (12 Gy) and media was immediately exchanged with fresh media containing 100 ng/mL MPL. After 24 hours, cells were harvested for qPCR analysis of polarization and activation markers (A). The capacity for serum derived antitumor antibodies to activate macrophages was tested using a co-culture system (B). Macrophages were cultured with PBS, MPL (100 ng/mL), serum from mice rendered disease free of B78 tumors via RT+C4+MPL treatment, or both MPL and serum. After 24 hours, cells were harvested for analysis of polarization (C), and activation markers (D). To test whether macrophages can be active in the presence of tumor cells, macrophages were cultured with or without 100 ng/mL MPL and 24 hours later B78 cells were added with or without serum from disease free mice. After 24 hours of co-culture macrophages were harvested for analysis of polarization (E) and activation markers (F). To confirm tumor specificity of the serum antibodies, this was repeated with the unrelated cell line Myc-CaP (G, H). One-way ANOVA with Tukey's honestly significant difference (HSD) test to adjust for multiple comparisons was used to assess statistical significance of observed mean differences in gene expression (significant differences, * $p < 0.05$, ** $p < 0.01$, *** $p < 0.001$, **** $p < 0.0001$). N=3 replicates per group. ANOVA, analysis of variance; MPL, monophosphoryl lipid; RT, radiation therapy.

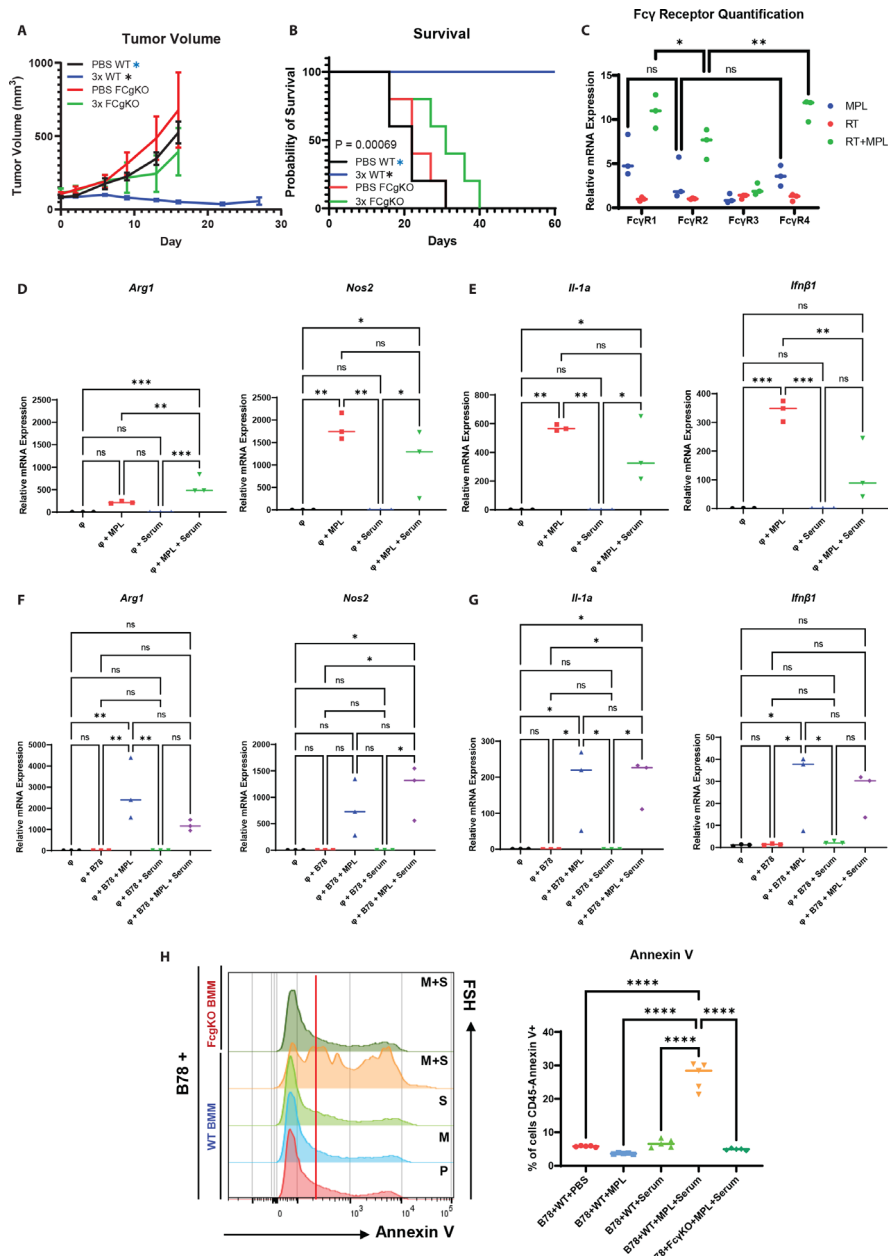


Figure 6 Serum antibody induced macrophage activation is dependent on Fc γ receptor and is critical for antitumor response. Significance of Fc γ receptor was tested in vivo. Wild-type (WT) and Fc γ receptor deficient mice were treated with either PBS or RT+C4+MPL (3x), and tumor growth and survival was tracked (A, B). N=5 mice per group. Bone marrow derived macrophages were radiated in culture (12 Gy) and media was immediately exchanged with fresh media containing 100 ng/mL MPL. After 24 hours cells were harvested for qPCR analysis of Fc γ receptor expression (C). To determine the importance of Fc γ receptor on macrophage activation, macrophages were cultured with PBS, MPL (100 ng/mL), serum from mice rendered disease free of B78 tumors via RT+C4+MPL treatment, or both MPL and serum. After 24 hours cells were harvested for analysis of polarization (D), and activation markers (E). To test whether macrophages can be active in the presence of tumor cells, macrophages were cultured with or without 100 ng/mL MPL and 24 hours later B78 cells were added with or without serum from disease free mice. After 24 hours of co-culture macrophages were harvested for analysis of polarization (F) and activation markers (G). N=3 replicates per group. To test whether serum derived antitumor antibodies can initiate ADCC, unstimulated and MPL stimulated macrophages were co-cultured with B78 cells with and without serum. After 24 hours cells were collected and analyzed via flow cytometry. CD45⁺Annexin V⁺ cells are plotted (H). n=5 replicates per group. One-way ANOVA with Tukey's honestly significant difference (HSD) test to adjust for multiple comparisons was used to assess statistical significance of observed mean differences in gene expression (significant differences, *p<0.05, **p<0.01, ***p<0.001, ****p<0.0001). Tumor growth was compared using linear mixed effects regression analysis with Tukey multiple comparisons testing. Kaplan-Meier estimation with log-rank testing and Cox regression were performed for survival analysis (significant differences, p<0.05, demarcated by * with the color of the asterisk representing which group from which the sample is significantly different). ANOVA, analysis of variance; MPL, monophosphoryl lipid; RT, radiation therapy; ADCC, antibody-dependent cellular cytotoxicity; PBS, phosphate buffered saline.

co-culture with B78 cells, did not significantly increase expression of either gene, nor did the addition of serum to MPL stimulated FcγR^{-/-} macrophages further increase expression compared with MPL stimulation alone (figure 6F). Similar trends were observed with activation markers *Il-1α* and *Ifnβ1* confirming that enhanced activation of macrophages following serum treatment of B78 tumors is reliant on Fcγ receptor expression (figure 6G).

To test whether serum antibodies can induce macrophage-mediated antibody-dependent cellular cytotoxicity, we co-cultured macrophages with B78 cells with and without MPL and serum. Using Annexin V staining as a marker of apoptosis, we observed a 5-fold increase in Annexin V staining in B78 cells co-cultured with macrophages stimulated with MPL and serum compared with stimulation with each agent alone or non-stimulated macrophages. The observed increase in Annexin V staining was lost when macrophages were deficient in Fcγ receptor (figure 6H).

Given the functional importance of the serum antibodies we then sought to determine the effects of our treatment regimen on B cells. We cultured B cells and treated them with either MPL, serum, MPL+serum, or PBS control. In separate experiments, we also cultured B cells and treated them with either RT, anti-CTLA-4, RT+ anti-CTLA-4, or PBS control. We observed no increase in B cell activation following MPL or serum treatment and only modest activation following RT (online supplemental figure S5B,C), suggesting B cells are not directly influenced by our treatment regimen.

MPL-induced immunity is dependent on Th1 cells

Given our observation that MPL can promote generation of antitumor antibodies, as well as directly activate macrophages which in turn can favor Th1 polarization of CD4 T cells and activation of CD8 T cells, we sought to determine which of these immune cells were critical for the antitumor response of combination RT+C4+MPL. We compared the efficacy of RT+MPL+C4 treatment in mice that were depleted of specific immune cell lineages by intraperitoneal injection of lineage-specific depleting antibodies. This included mice depleted of macrophages (αCD115), NK cells (αNK1.1), CD4 T cells (αCD4), CD8 T cells (αCD8), or both CD4 and CD8 T cells (αCD4/CD8). The loss of macrophages and CD4 cells significantly reduced the antitumor response compared with non-depleted mice. Interestingly, loss of NK and CD8 cells each had no effect on antitumor response (figure 7A) nor overall survival (figure 7B).

We collected serum at day 15 following RT for antitumor antibody quantification as done previously. We again observed a significant increase in the IgG2c:IgG1 ratio with combination RT+C4+MPL compared with PBS control. Depletion of NK cells or CD8 T cells had no effect on the IgG2c:IgG1 ratio, whereas macrophage depletion and CD4 T cell depletion significantly reduced the IgG2c:IgG1 ratio compared with

combination RT+C4+MPL suggesting Th1 associated antitumor antibody class switching is dependent on both macrophages and CD4 T cells (figure 7C). Interestingly, depletion of CD4 T cells significantly reduced production of total IgG suggesting that antitumor antibody production is dependent, at least in part, on CD4 T cells (figure 7D).

We hypothesized that ablation of Th1 cells specifically was responsible for the loss of treatment efficacy when CD4 cells were depleted. To test this we compared the antitumor efficacy of combination RT+C4+MPL in wild-type and TBET^{-/-} mice. TBET deficiency abrogated the antitumor response and generation of Th1 associated antitumor antibodies following RT+C4+MPL treatment compared to wild-type mice (figure 7E,F). We observed a significant reduction in intratumoral CD4 cell infiltration and M1:M2 macrophage ratio in TBET^{-/-} mice compared with wild-type (figure 7G). In addition, within the tumor draining lymph node we observed a significant reduction in Th1 CD4 T cells and IFNγ⁺ CD4 T cells in TBET^{-/-} mice compared with wild-type (figure 7H). Taken together, these data suggest Th1 CD4 T cells are central to the mechanism underlying generation of antitumor immunity with combination RT+C4+MPL.

MPL treatment promotes systemic immunity independent of CD8 T cells

Given that loss of CD8 cells had no effect on the antitumor response, we sought to determine whether CD8 cells were required for generation of systemic immunity. We used a systemic disease model consisting of a B78 primary tumor as well as intravenously injected B16 melanoma cells to model heterogeneous metastatic disease. B16 cells are parental to B78 and share common tumor neo-antigens that can be recognized by T cells.^{6 28 38} Treatment with RT+MPL+C4 significantly reduced growth at the primary tumor and significantly increased survival compared with RT+C4 (figure 8A,B). Immediately following death or at day 60, lungs were collected to determine metastatic burden. The addition of MPL significantly reduced lung metastatic burden compared with RT+C4 (figure 8C). Interestingly, the enhanced antitumor response, survival, and decreased lung metastasis burden observed with RT+C4+MPL was independent of CD8 T cells (figure 8A–C). Recent evidence suggests that CD4 cells may directly kill tumor cells through MHC-II mediated recognition.³⁹ We measured expression of MHC-II on B16 tumor cells *in vitro* following RT as well as *in vivo* following combination RT+C4+MPL and in either case observed a down-regulation of MHC-II expression compared with PBS control (online supplemental figure S5D,E). In addition, we isolated CD4 cells from B16 tumor bearing mice at day 15 following RT+C4+MPL treatment and co-cultured them with B16 melanoma cells. We observed no change in tumor cell killing compared with CD4 cells isolated from tumor bearing mice treated with PBS

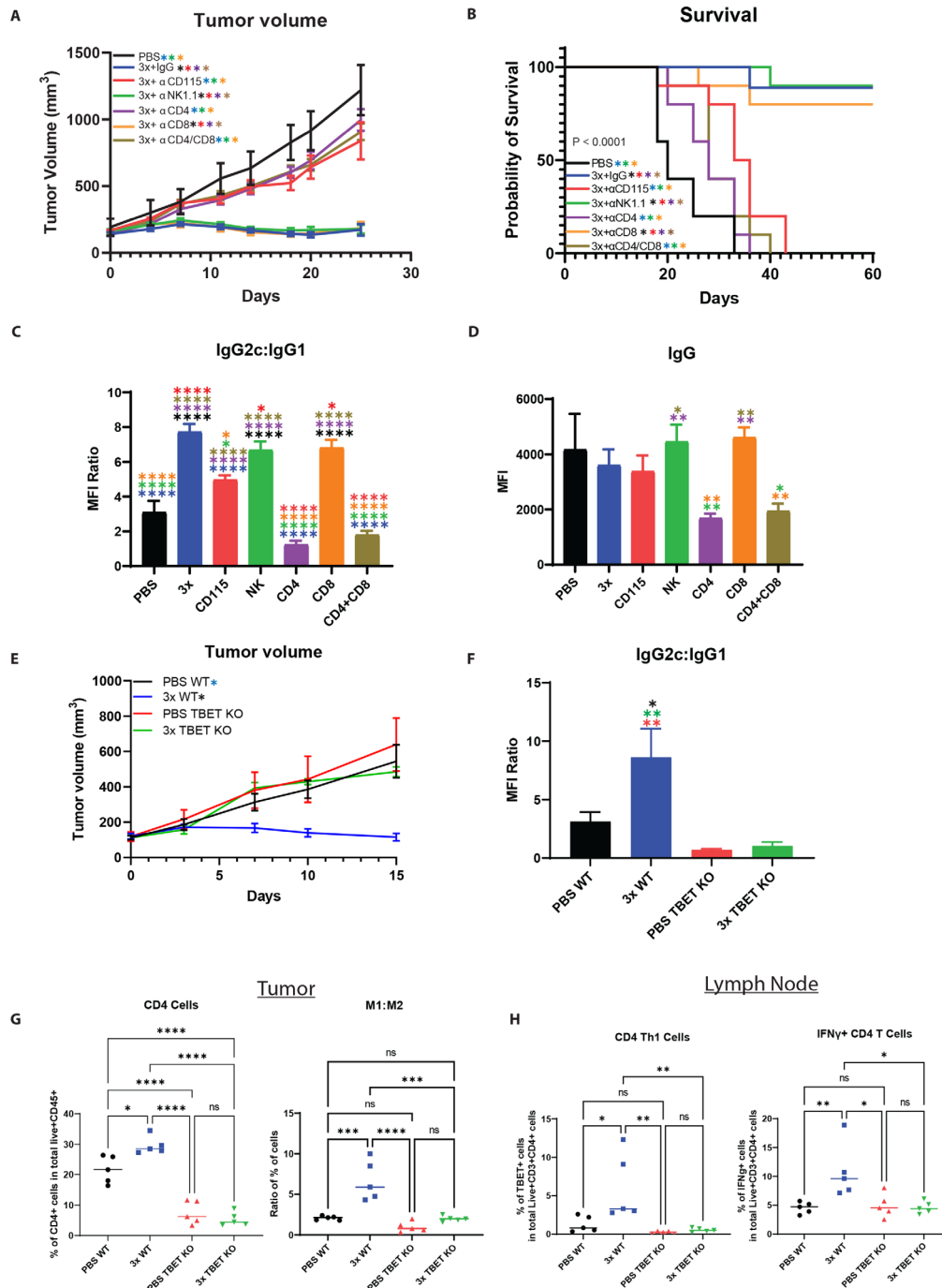


Figure 7 MPL-induced immune response is dependent on macrophages and Th1 CD4 T cells. Importance of different immune cell populations for the antitumor response generated via RT+C4+MPL was determined using antibody-based depletion. Mice bearing B78 tumors were treated with either PBS or RT+C4+MPL (3x) and either macrophages (α CD115), NK cells (α NK1.1), CD4 T cells (α CD4), CD8 T cells (α CD8), or both CD4 and CD8 T cells (α CD/CD8) were depleted, and tumor growth and survival was tracked (A, B). N=5–10 mice per group. At day 15 following RT, serum was collected for antitumor antibody quantification (C, D). Importance of Th1 CD4 T cells for the antitumor response generated via RT+C4+MPL was determined using TBET deficient mice. Wild-type and TBET deficient mice (TBET KO) were treated with either PBS or RT+C4+MPL (3x), and tumor growth was tracked (E). N=5 mice per group. At day 15 following RT, serum was collected for antitumor antibody quantification (F) and tumor and draining lymph node were collected for infiltration analysis (G, H). Tumor growth was compared using linear mixed effects regression analysis with Tukey multiple comparisons testing. Kaplan-Meier estimation with log-rank testing and Cox regression were performed for survival analysis (significant differences, $p < 0.05$, demarcated by * with the color of the asterisk representing which group from which the sample is significantly different). One-way ANOVA with Tukey's honestly significant difference (HSD) test to adjust for multiple comparisons was used to assess statistical significance of observed mean differences in lung metastases (significant differences, * $p < 0.05$, ** $p < 0.01$, *** $p < 0.001$, **** $p < 0.0001$, with color of asterisk representing which group from which the sample is significantly different). ANOVA, analysis of variance; MFI, median fluorescence intensity; MPL, monophosphoryl lipid; RT, radiation therapy; TBET, T-box transcription factor 21.

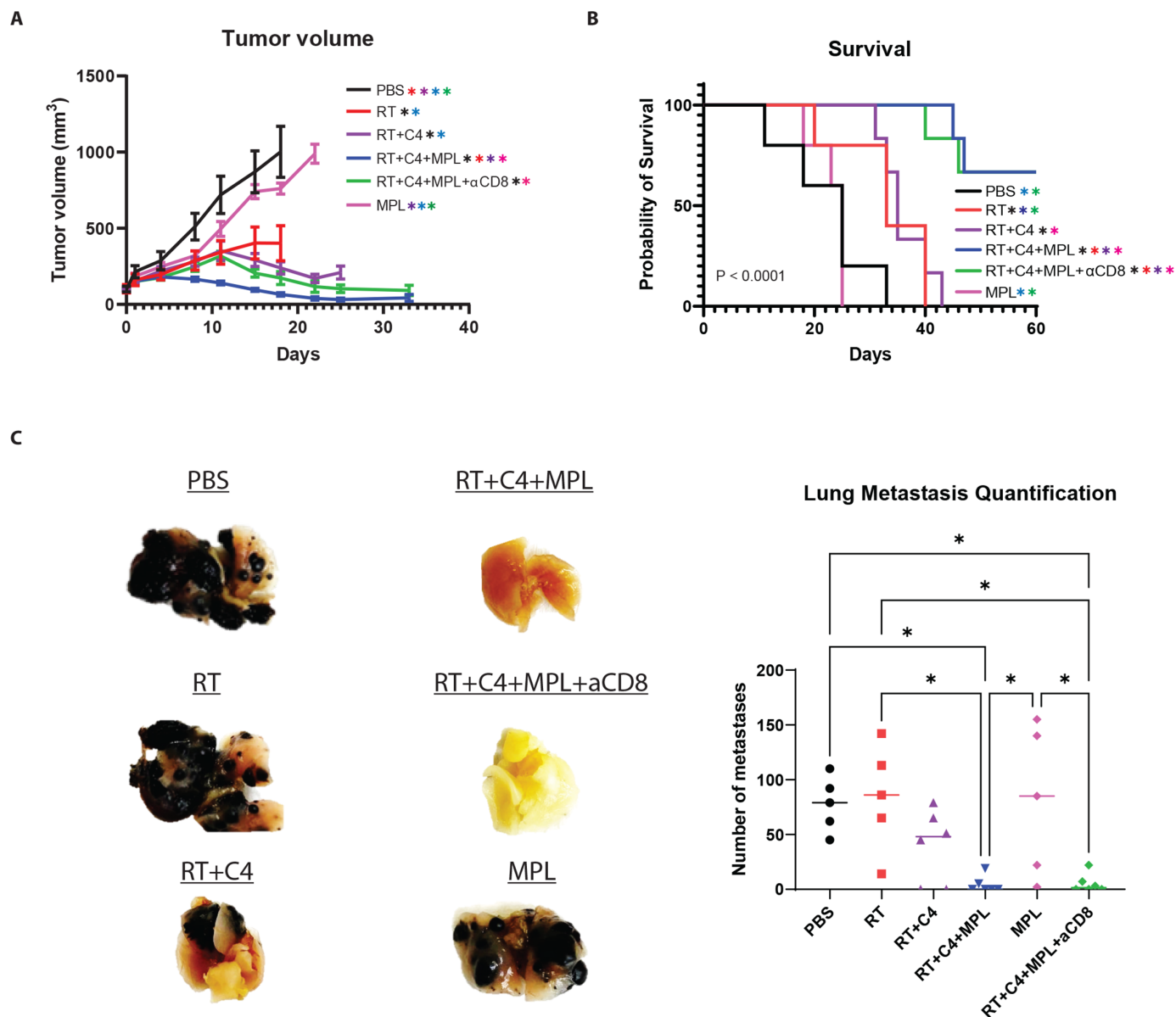


Figure 8 MPL enhances systemic immune response independent of CD8 T cells. To determine whether CD8 T cells were required for generation of systemic immune response, mice bearing B78 primary tumors and B16 lung metastases (250 000 B16 cells injected via tail vein immediately following RT) were treated with either PBS, RT, RT+C4, RT+C4+MPL, or MPL. In addition, a separate cohort of mice treated with RT+C4+MPL were also treated with CD8 depletion antibody. Tumor volume and survival were tracked (A, B). At time of death or day 60 following treatment initiation, lungs were removed and number of metastases were calculated (C). N=5–6 mice per group. Tumor growth was compared using linear mixed effects regression analysis with Tukey multiple comparisons testing. Kaplan-Meier estimation with log-rank testing and Cox regression were performed for survival analysis (significant differences, $p < 0.05$, demarcated by * with the color of the asterisk representing which group from which the sample is significantly different). One-way ANOVA with Tukey's honestly significant difference (HSD) test to adjust for multiple comparisons was used to assess statistical significance of observed mean differences in lung metastases (significant differences, * $p < 0.05$, ** $p < 0.01$, *** $p < 0.001$, **** $p < 0.0001$, with color of asterisk representing which group from which the sample is significantly different). ANOVA, analysis of variance; MPL, monophosphoryl lipid; RT, radiation therapy; PBS, phosphate buffered saline.

control (online supplemental figure S5F). Together, these data suggest macrophages are the primary cytotoxic cell activated by combination treatment.

DISCUSSION

We have demonstrated that intratumoral injection of the vaccine adjuvant MPL can augment the antitumor

immune response generated by RT and thereby augment response to anti-CTLA-4 checkpoint blockade. This resulted from favorable effects of MPL on polarization of both M1 macrophages and Th1 CD4 T cells in the radiated tumor microenvironment. Consistent with Th1 CD4 T cell polarization, we observed that MPL induced production of IgG2c dominant antitumor antibodies as well as

upregulation of the IgG2c high-affinity Fc γ receptors I and IV on macrophages. MPL-stimulated macrophages exposed to antitumor antibodies on tumor cells exhibited increased activation and direct killing of tumor cells *in vitro*. Depletion of macrophages, Th1 CD4 T cells, or loss of Fc γ receptor expression completely abrogated the anti-tumor immune response *in vivo*. Lastly, we demonstrate the capacity of our combination treatment regimen to generate local and systemic immune responses through a CD8 T cell independent mechanism.

Our findings report generation of a CD8 independent systemic immune response that is dependent on both Th1 CD4 T cells and macrophages. These suggest that CD4 T cell polarization toward a Th1 phenotype is required to generate functional antitumor antibodies that are IgG2c subclass dominant. We demonstrate that these antibodies have the potential to enable macrophage mediated tumor cell killing *in vitro* and *in vivo* but only when macrophages have been stimulated with MPL. Interestingly, loss of natural killer cells *in vivo* did not abrogate the anti-tumor immune response despite their ability to generate antibody dependent cell-mediated cytotoxicity. This may be at least partially explained by the observation that NK cells express relatively low amounts of TLR4 compared with macrophages,⁴⁰ and that based on our data, functional antibody recognition in this model system requires MPL stimulation.

Prior studies have suggested potential benefit of combining MPL with checkpoint blockade. In preclinical models MPL has been shown to increase the antitumor efficacy of anti-PD-1/anti-PD-L1 therapy through activation of dendritic cells and enhanced antigen presentation.^{41 42} Within the tumor draining lymph node, we observed a significant increase in dendritic cell activation following combination radiation and anti-CTLA-4, which is consistent with prior reports.^{21 43} However, the addition of MPL did not further increase dendritic cell activation, suggesting that the role of MPL in our treatment regimen extends beyond supporting antigen presentation.

As a general class of immune adjuvants, TLR4 agonists have gained interest in testing their potential to enhance conventional vaccine efficacy, namely through promotion of Th1 polarization.⁴⁴ In our model, we observed a significant increase in Th1 polarization when MPL was added to RT and anti-CTLA-4, but not as a single agent. Interestingly, the depth of response to treatment positively correlated with magnitude of Th1 polarization as measured by IgG2c class switching. The magnitude of IgG2c class switching was significantly increased in mice developing a CR, but only when MPL was added to RT and anti-CTLA-4. This is in contrast to prior reports demonstrating that anti-CTLA-4 enables expansion of Th1-like CD4 T cell populations.^{45 46} However, it is notable that these studies were conducted in the MC-38 colon carcinoma model, which possesses relatively high immunogenicity. Additionally, the authors confirmed these findings in the poorly immunogenic B16 melanoma model, which

is the parental cell line to our B78 melanoma model, but required treatment with the GVAX tumor vaccine in order to boost overall T cell infiltration to enable their analyses. This overall lack of T cell infiltration could at least partially explain the lack of observed Th1 polarization with combination RT and anti-CTLA-4 in our models.

Our observations describe the importance of endogenously generated antitumor antibody class dominance and recognition through macrophage Fc γ receptor binding in generating a successful antitumor immune response. Four individual Fc γ receptors have been identified in mice, with all four being expressed on macrophages. The receptors Fc γ R1 and Fc γ R4 have a high affinity for the antibody subclass IgG2c only, whereas Fc γ R2 and Fc γ R3 have a low affinity for both IgG2c and IgG1.⁴⁷ Given our combination treatment results in antibody populations that significantly favor IgG2c over IgG1, these antitumor antibodies selectively stimulate the activating receptors Fc γ R1 and Fc γ R4, of which the expression of these are increased with MPL treatment, and further increased with the addition of RT. These mechanisms may underly the observed synergy between MPL and combination RT and anti-CTLA-4.

We acknowledge several limitations of this study which include the use of syngeneic heterotopic murine tumor models that may not fully recapitulate the tumor heterogeneity nor the immune microenvironment that is observed in humans. Although our findings in two separate syngeneic tumor models of melanoma and prostate cancer suggest that the addition of MPL to combination RT and anti-CTLA-4 is a promising treatment strategy, others have previously shown that syngeneic tumor models can possess pre-existing immunity that is critical for the response to RT and immune checkpoint inhibition.^{48 49} Therefore, additional studies with this combination treatment strategy in spontaneously developing murine tumor models would further support the potential for successful clinical translation. A similar limitation arises from the observation that anti-CTLA-4 generates superior immune responses compared with anti-PD-1/L1 therapies in many murine tumor models, likely due, at least in part, to regulatory T cell depletion generated via CTLA-4 blockade. This directly contrasts with clinical studies and further highlights key differences between murine and human immunity. To overcome this limitation and test whether MPL may enhance the antitumor immune response to combination RT and anti-CTLA-4, we have focused our efforts on utilizing poorly immunogenic murine tumor models that do not respond well to anti-CTLA-4 monotherapy. For RT treatment, we used a single fraction of 12 Gy based on our previous data in the B78 tumor model, however, we did not test other RT doses or fractionation schemes of which may influence treatment efficacy. Future work dedicated to testing MPL in combination with other RT modalities, doses, and fractionation schemes will be necessary to fully determine the translational potential of MPL treatment in the context of RT. Lastly, our treatment strategy involves the intratumoral administration of MPL

which may limit translational potential. However, several immunotherapy regimens are currently in development that use intratumoral approaches to delivery.⁵⁰ In addition, advances in image guidance within the field of interventional radiology may enable translation to a broad range of cancer types.

There is rapidly growing interest in developing ISV strategies that incorporate RT. To date there are nearly 600 active trials that are investigating radiation in combination with anti-CTLA-4 or PD-1/L1 checkpoint blockade.⁵¹ In addition to checkpoint blockade, a variety of other immunotherapies are under investigation including cytokines such as IL-2 and IL-15, cell-based therapies such as CAR-T cells, cancer vaccines, oncolytic viruses, and antibody agonists such as anti-OX40 and anti-GITR. Each of these ISV strategies may benefit from combination with additional adjuvants such as MPL, and further preclinical and clinical studies are warranted to fully investigate the potential of combination therapy strategies.

Author affiliations

¹Department of Human Oncology, University of Wisconsin-Madison School of Medicine and Public Health, Madison, Wisconsin, USA

²Department of Biostatistics and Medical Informatics, University of Wisconsin-Madison School of Medicine and Public Health, Madison, Wisconsin, USA

³Department of Pediatrics, University of Wisconsin-Madison School of Medicine and Public Health, Madison, Wisconsin, USA

Acknowledgements The authors would like to thank the University of Wisconsin Carbone Cancer Center (UWCCC) for support of this project, and colleagues Amy Erbe, PhD, and Alexander Rakhmilevich, MD PhD, for many helpful discussions. The authors would also like to acknowledge the University of Wisconsin Small Animal Imaging and Radiotherapy Facility. Study schema figures were generated using BioRender.com.

Contributors Conceptualization: JCJ and ZSM. Methodology: JCJ and WJJ. Investigation: JCJ, WJJ, AMB, PAC, RNS, IC and EJN. Visualization: JCJ and WJJ. Statistical analysis: JCJ, TCH and KK. Funding acquisition: ZSM. Supervision: ZSM, WJJ, PMS, KK. Writing—original draft: JCJ. Writing—review and editing: JCJ, PMS, and ZSM. Guarantor: ZSM.

Funding This project funded by National Institutes of Health grant P30 CA014520 National Institutes of Health grant P50 DE026787 National Institutes of Health grant 1DP50D024576 (ZSM) National Institutes of Health grant U01CA233102 (ZSM) National Institutes of Health grant P01CA250972 (ZSM) National Institutes of Health grant T32GM140935 National Institutes of Health grant TL1TR002375 (JCJ) National Institutes of Health grant F30CA250263 (JCJ) National Institutes of Health grant R35CA197078 (PMS).

Competing interests ZSM has financial interest in Archeus Technologies. ZSM is a member of the Scientific Advisory Boards for Archeus Technologies and for Seneca Therapeutics. Based on the results presented herein, ZSM and JCJ are inventors on a filed patent that is managed by the Wisconsin Alumni Research Foundation relating to the use of MPL as an adjuvant for in situ vaccines. ZSM and PMS are inventors on patents or filed patents managed by the Wisconsin Alumni Research Foundation relating to mAb-related or nanoparticle immunotherapies and the interaction of targeted radionuclide therapies and immunotherapies.

Patient consent for publication Not applicable.

Ethics approval Mice were housed and treated under a protocol (protocol number M005670) approved by the Institutional Animal Care and Use Committee (IACUC) at the University of Wisconsin – Madison.

Provenance and peer review Not commissioned; externally peer reviewed.

Data availability statement All data relevant to the study are included in the article or uploaded as online supplemental information.

Supplemental material This content has been supplied by the author(s). It has not been vetted by BMJ Publishing Group Limited (BMJ) and may not have been

peer-reviewed. Any opinions or recommendations discussed are solely those of the author(s) and are not endorsed by BMJ. BMJ disclaims all liability and responsibility arising from any reliance placed on the content. Where the content includes any translated material, BMJ does not warrant the accuracy and reliability of the translations (including but not limited to local regulations, clinical guidelines, terminology, drug names and drug dosages), and is not responsible for any error and/or omissions arising from translation and adaptation or otherwise.

Open access This is an open access article distributed in accordance with the Creative Commons Attribution Non Commercial (CC BY-NC 4.0) license, which permits others to distribute, remix, adapt, build upon this work non-commercially, and license their derivative works on different terms, provided the original work is properly cited, appropriate credit is given, any changes made indicated, and the use is non-commercial. See <http://creativecommons.org/licenses/by-nc/4.0/>.

ORCID iDs

Justin C Jagodinsky <http://orcid.org/0000-0002-6204-4899>

Paul A Clark <http://orcid.org/0000-0002-1608-1146>

Paul M Sondel <http://orcid.org/0000-0002-0981-8875>

REFERENCES

- Bernier J, Hall EJ, Giaccia A. Radiation oncology: a century of achievements. *Nat Rev Cancer* 2004;4:737–47.
- Golden EB, Frances D, Pellicciotta I, et al. Radiation fosters dose-dependent and chemotherapy-induced immunogenic cell death. *Oncoimmunology* 2014;3:e28518.
- Golden EB, Apetoh L. Radiotherapy and immunogenic cell death. *Semin Radiat Oncol* 2015;25:11–17.
- Demaria S, Bhardwaj N, McBride WH, et al. Combining radiotherapy and immunotherapy: a revived partnership. *Int J Radiat Oncol Biol Phys* 2005;63:655–66.
- Werner LR, Kler JS, Gressett MM, et al. Transcriptional-mediated effects of radiation on the expression of immune susceptibility markers in melanoma. *Radiother Oncol* 2017;124:418–26.
- Morris ZS, Guy El, Francis DM, et al. In situ tumor vaccination by combining local radiation and tumor-specific antibody or immunocytokine treatments. *Cancer Res* 2016;76:3929–41.
- Campbell BB, Light N, Fabrizio D, et al. Comprehensive analysis of hypermutation in human cancer. *Cell* 2017;171:1042–56.
- Formenti SC, Rudqvist N-P, Golden E, et al. Radiotherapy induces responses of lung cancer to CTLA-4 blockade. *Nat Med* 2018;24:1845–51.
- Kachikwu EL, Iwamoto KS, Liao Y-P, et al. Radiation enhances regulatory T cell representation. *Int J Radiat Oncol Biol Phys* 2011;81:1128–35.
- Tsai C-S, Chen F-H, Wang C-C, et al. Macrophages from irradiated tumors express higher levels of iNOS, arginase-I and COX-2, and promote tumor growth. *Int J Radiat Oncol Biol Phys* 2007;68:499–507.
- Liang H, Deng L, Hou Y, et al. Host STING-dependent MDSC mobilization drives extrinsic radiation resistance. *Nat Commun* 2017;8:1736.
- Korman AJ, Peggs KS, Allison JP. Checkpoint blockade in cancer immunotherapy. *Adv Immunol* 2006;90:297–339.
- Galon J, Bruni D. Approaches to treat immune hot, altered and cold tumours with combination immunotherapies. *Nat Rev Drug Discov* 2019;18:197–218.
- Hodi FS, Chiarion-Sileni V, Gonzalez R, et al. Nivolumab plus ipilimumab or nivolumab alone versus ipilimumab alone in advanced melanoma (CheckMate 067): 4-year outcomes of a multicentre, randomised, phase 3 trial. *Lancet Oncol* 2018;19:1480–92.
- Kather JN, Suarez-Carmona M, Charoentong P, et al. Topography of cancer-associated immune cells in human solid tumors. *Elife* 2018;7. doi:10.7554/eLife.36967. [Epub ahead of print: 04 Sep 2018].
- Kwon ED, Drake CG, Scher HI, et al. Ipilimumab versus placebo after radiotherapy in patients with metastatic castration-resistant prostate cancer that had progressed after docetaxel chemotherapy (CA184-043): a multicentre, randomised, double-blind, phase 3 trial. *Lancet Oncol* 2014;15:700–12.
- Mapara MY, Sykes M. Tolerance and cancer: mechanisms of tumor evasion and strategies for breaking tolerance. *J Clin Oncol* 2004;22:1136–51.
- Deng L, Liang H, Burnette B, et al. Irradiation and anti-PD-L1 treatment synergistically promote antitumor immunity in mice. *J Clin Invest* 2014;124:687–95.
- Twyman-Saint Victor C, Rech AJ, Maity A, et al. Radiation and dual checkpoint blockade activate non-redundant immune mechanisms in cancer. *Nature* 2015;520:373–7.

- 20 Demaria S, Ng B, Devitt ML, *et al.* Ionizing radiation inhibition of distant untreated tumors (abscopal effect) is immune mediated. *Int J Radiat Oncol Biol Phys* 2004;58:862–70.
- 21 Dewan MZ, Galloway AE, Kawashima N, *et al.* Fractionated but not single-dose radiotherapy induces an immune-mediated abscopal effect when combined with anti-CTLA-4 antibody. *Clin Cancer Res* 2009;15:5379–88.
- 22 Formenti SC, Demaria S. Systemic effects of local radiotherapy. *Lancet Oncol* 2009;10:718–26.
- 23 Rudqvist N-P, Pilonis KA, Lhuillier C, *et al.* Radiotherapy and CTLA-4 blockade shape the TCR repertoire of tumor-infiltrating T cells. *Cancer Immunol Res* 2018;6:139–50.
- 24 McBride SM, Sherman EJ, Tsai CJ, *et al.* A phase II randomized trial of nivolumab with stereotactic body radiotherapy (SBRT) versus nivolumab alone in metastatic (M1) head and neck squamous cell carcinoma (HNSCC). *Journal of Clinical Oncology* 2018;36:6009.
- 25 Theelen WSME, Peulen HMU, Lalezari F, *et al.* Effect of pembrolizumab after stereotactic body radiotherapy vs pembrolizumab alone on tumor response in patients with advanced non-small cell lung cancer: results of the PEMBRO-RT phase 2 randomized clinical trial. *JAMA Oncol* 2019;5:1276–1282.
- 26 Wang Y-Q, Bazin-Lee H, Evans JT, *et al.* Mpl adjuvant contains competitive antagonists of human TLR4. *Front Immunol* 2020;11:577823.
- 27 Centers for Disease Control and Prevention (CDC). Fda licensure of bivalent human papillomavirus vaccine (HPV2, Cervarix) for use in females and updated HPV vaccination recommendations from the Advisory Committee on immunization practices (ACIP). *MMWR Morb Mortal Wkly Rep* 2010;59:626–9.
- 28 Haraguchi M, Yamashiro S, Yamamoto A, *et al.* Isolation of GD3 synthase gene by expression cloning of GM3 alpha-2,8-sialyltransferase cDNA using anti-GD2 monoclonal antibody. *Proc Natl Acad Sci U S A* 1994;91:10455–9.
- 29 Bauché D, Joyce-Shaikh B, Jain R, *et al.* LAG3⁺ Regulatory T Cells Restrain Interleukin-23-Producing CX3CR1⁺ Gut-Resident Macrophages during Group 3 Innate Lymphoid Cell-Driven Colitis. *Immunity* 2018;49:e345.
- 30 Baniel CC, Heinze CM, Hoefges A, *et al.* *In situ* Vaccine Plus Checkpoint Blockade Induces Memory Humoral Response. *Front Immunol* 2020;11:1610.
- 31 Manzanero S. Generation of mouse bone marrow-derived macrophages. *Methods Mol Biol* 2012;844:177–81.
- 32 Jin WJ, Erbe AK, Schwarz CN, *et al.* Tumor-Specific Antibody, Cetuximab, Enhances the *In Situ* Vaccine Effect of Radiation in Immunologically Cold Head and Neck Squamous Cell Carcinoma. *Front Immunol* 2020;11:591139.
- 33 Jagodinsky JC, Jin WJ, Bates AM, *et al.* Temporal analysis of type 1 interferon activation in tumor cells following external beam radiotherapy or targeted radionuclide therapy. *Theranostics* 2021;11:6120–37.
- 34 Topalian SL, Hodi FS, Brahmer JR, *et al.* Safety, activity, and immune correlates of anti-PD-1 antibody in cancer. *N Engl J Med* 2012;366:2443–54.
- 35 Beer TM, Kwon ED, Drake CG, *et al.* Randomized, double-blind, phase III trial of ipilimumab versus placebo in asymptomatic or minimally symptomatic patients with metastatic Chemotherapy-Naive castration-resistant prostate cancer. *J Clin Oncol* 2017;35:40–7.
- 36 Nazeri S, Zakeri S, Mehrizi AA, *et al.* Measuring of IgG2c isotype instead of IgG2a in immunized C57BL/6 mice with Plasmodium vivax trap as a subunit vaccine candidate in order to correct interpretation of Th1 versus Th2 immune response. *Exp Parasitol* 2020;216:107944.
- 37 De Filippo K, Dudeck A, Hasenberg M, *et al.* Mast cell and macrophage chemokines CXCL1/CXCL2 control the early stage of neutrophil recruitment during tissue inflammation. *Blood* 2013;121:4930–7.
- 38 Clark PA, Sriramaneni RN, Jin WJ, *et al.* *In situ* vaccination at a peripheral tumor site augments response against melanoma brain metastases. *J Immunother Cancer* 2020;8.
- 39 Oh DY, Fong L. Cytotoxic CD4⁺ T cells in cancer: Expanding the immune effector toolbox. *Immunity* 2021;54:2701–11.
- 40 Hornung V, Rothenfusser S, Britsch S, *et al.* Quantitative expression of Toll-like receptor 1–10 mRNA in cellular subsets of human peripheral blood mononuclear cells and sensitivity to CpG oligodeoxynucleotides. *J Immunol* 2002;168:4531–7.
- 41 Jeong Y, Kim GB, Ji Y, *et al.* Dendritic cell activation by an E. coli-derived monophosphoryl lipid A enhances the efficacy of PD-1 blockade. *Cancer Lett* 2020;472:19–28.
- 42 Zhang W, Lim S-M, Hwang J, *et al.* Monophosphoryl lipid A-induced activation of plasmacytoid dendritic cells enhances the anti-cancer effects of anti-PD-L1 antibodies. *Cancer Immunol Immunother* 2021;70:689–700.
- 43 Demaria S, Kawashima N, Yang AM, *et al.* Immune-Mediated inhibition of metastases after treatment with local radiation and CTLA-4 blockade in a mouse model of breast cancer. *Clin Cancer Res* 2005;11:728–34.
- 44 Orr MT, Duthie MS, Windish HP, *et al.* Myd88 and TRIF synergistic interaction is required for TH1-cell polarization with a synthetic TLR4 agonist adjuvant. *Eur J Immunol* 2013;43:2398–408.
- 45 Wei SC, Levine JH, Cogdill AP, *et al.* Distinct cellular mechanisms underlie anti-CTLA-4 and anti-PD-1 checkpoint blockade. *Cell* 2017;170:e1117:1120–33.
- 46 Wei SC, Anang N-AAS, Sharma R, *et al.* Combination anti-CTLA-4 plus anti-PD-1 checkpoint blockade utilizes cellular mechanisms partially distinct from monotherapies. *Proc Natl Acad Sci U S A* 2019;116:22699–709.
- 47 Bruhns P. Properties of mouse and human IgG receptors and their contribution to disease models. *Blood* 2012;119:5640–9.
- 48 Wisdom AJ, Mowery YM, Hong CS, *et al.* Single cell analysis reveals distinct immune landscapes in transplant and primary sarcomas that determine response or resistance to immunotherapy. *Nat Commun* 2020;11:6410.
- 49 Crittenden MR, Zebertavage L, Kramer G, *et al.* Tumor cure by radiation therapy and checkpoint inhibitors depends on pre-existing immunity. *Sci Rep* 2018;8:7012.
- 50 Aznar MA, Tinari N, Rullán AJ, *et al.* Intratumoral delivery of Immunotherapy-Act locally, think globally. *J Immunol* 2017;198:31–9.
- 51 Jagodinsky JC, Harari PM, Morris ZS. The promise of combining radiation therapy with immunotherapy. *Int J Radiat Oncol Biol Phys* 2020;108:6–16.